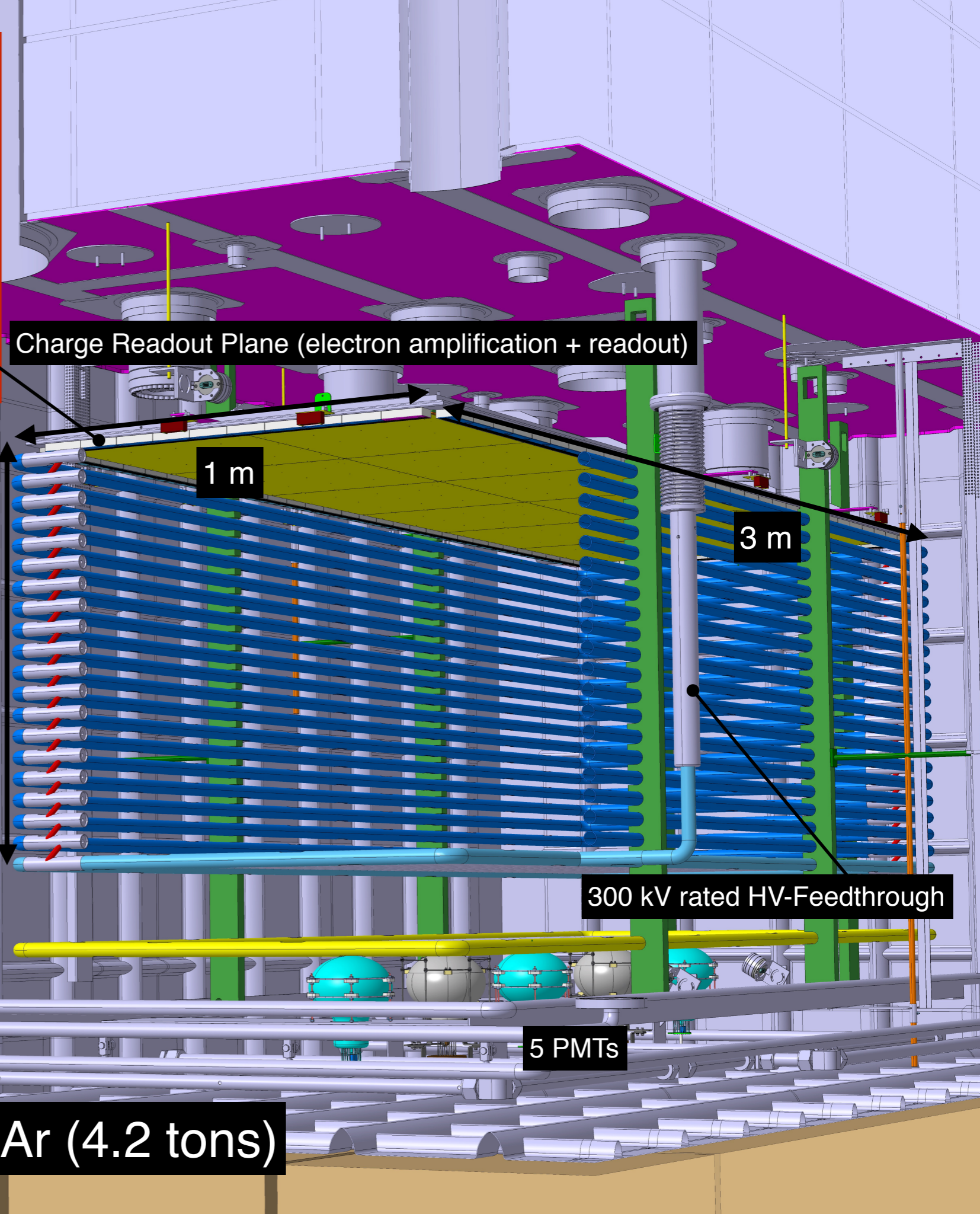
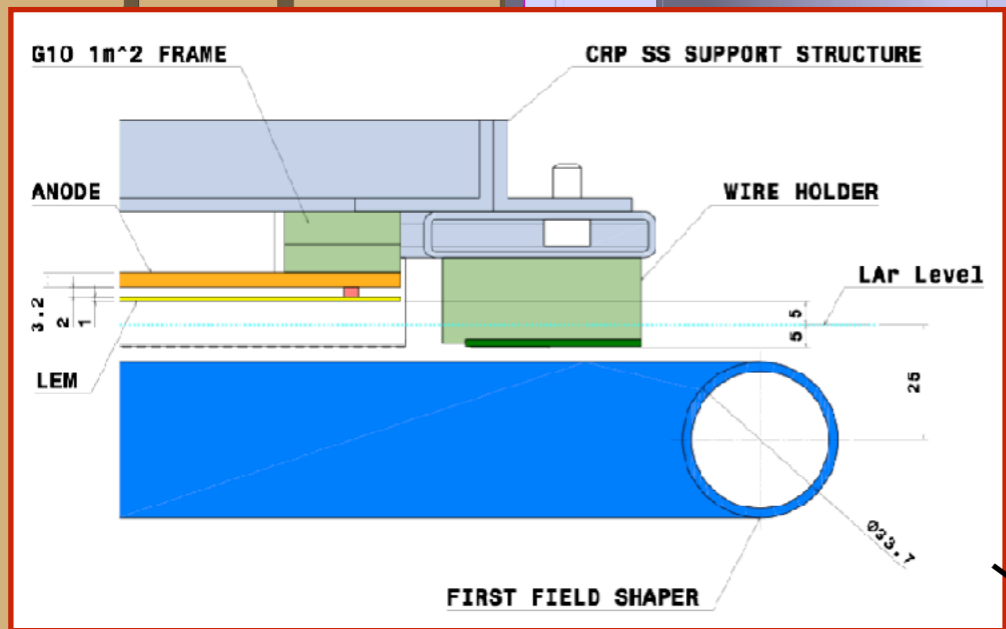


# Results from the 3x1x1 m<sup>3</sup> demonstrator

Sebastien Murphy

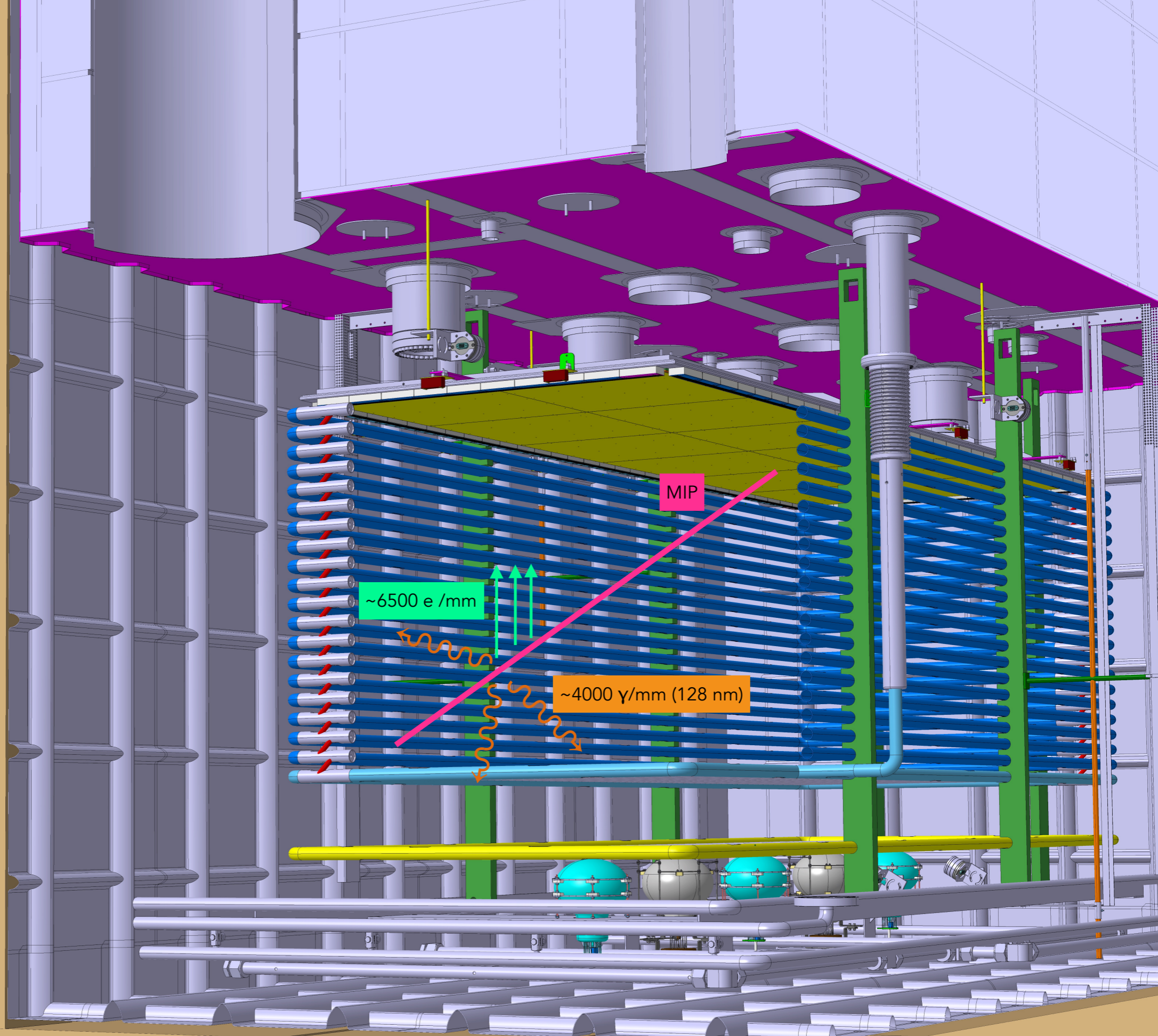
LBNC meeting, CERN Nov 2018



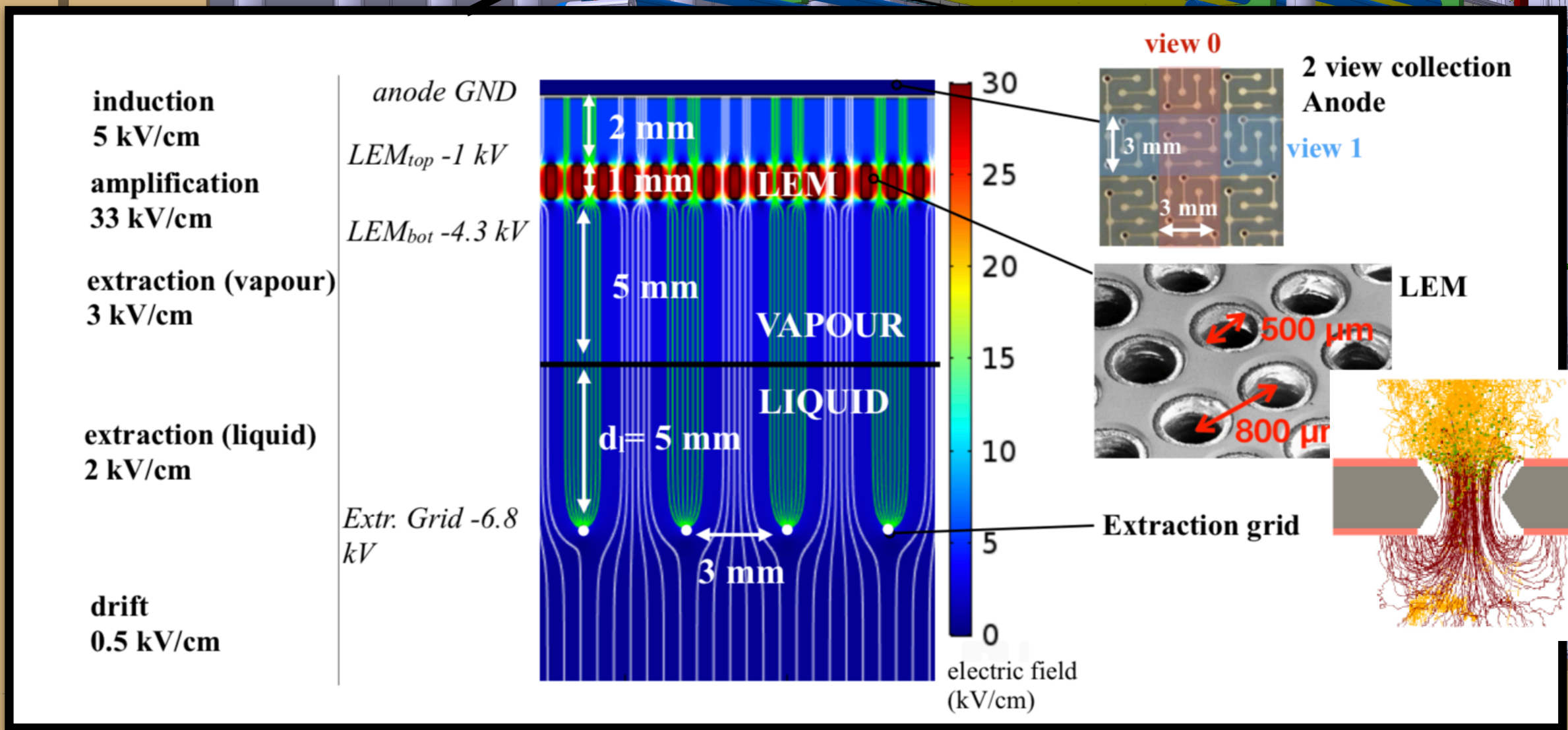
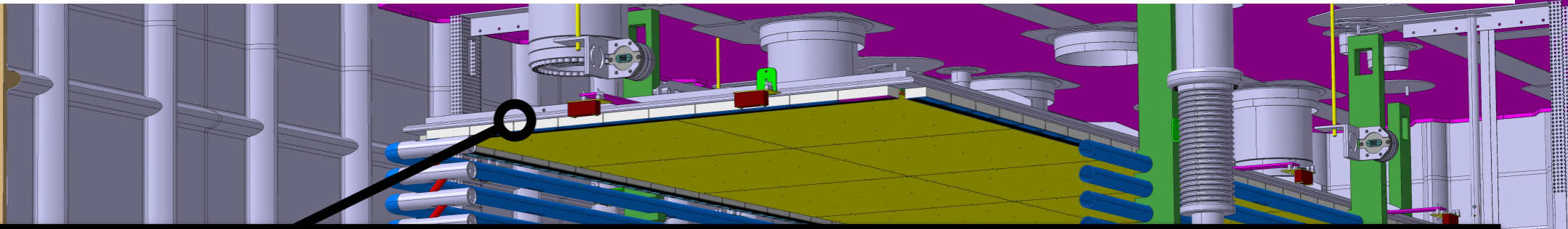


1 m passive insulation

3x1x1 m<sup>3</sup> active LAr (4.2 tons)



- drifting charges are extracted from the liquid to the vapour phase by an electric field in the liquid of around 2 kV/cm
- the charges once in pure argon vapour are multiplied inside 50x50 cm<sup>2</sup> area LEMs (Large Electron Multipliers) assembled side by side
- the amplified charges are collected on a 2D segmented anode



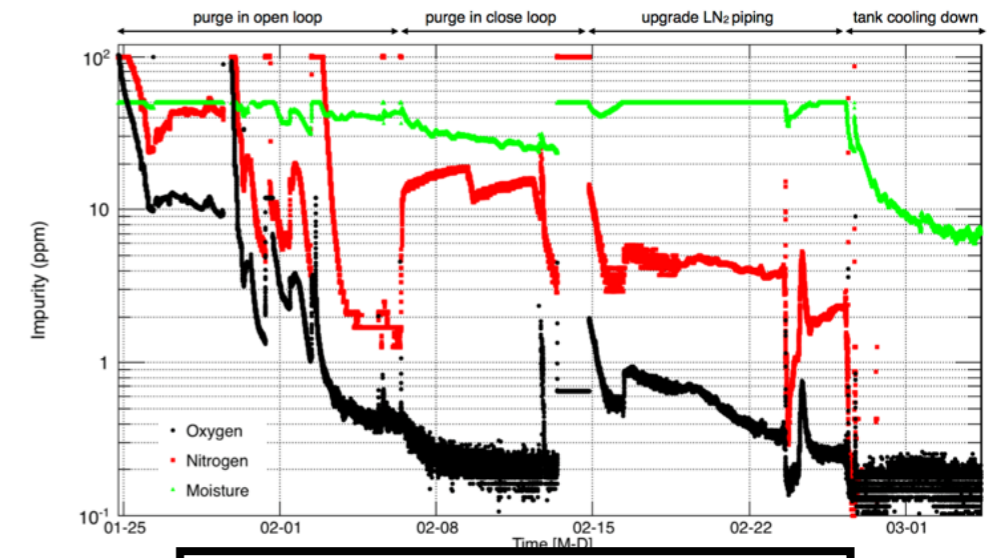
# 3x1x1 construction 2015-2016



**2015 - Cryostat constructed**



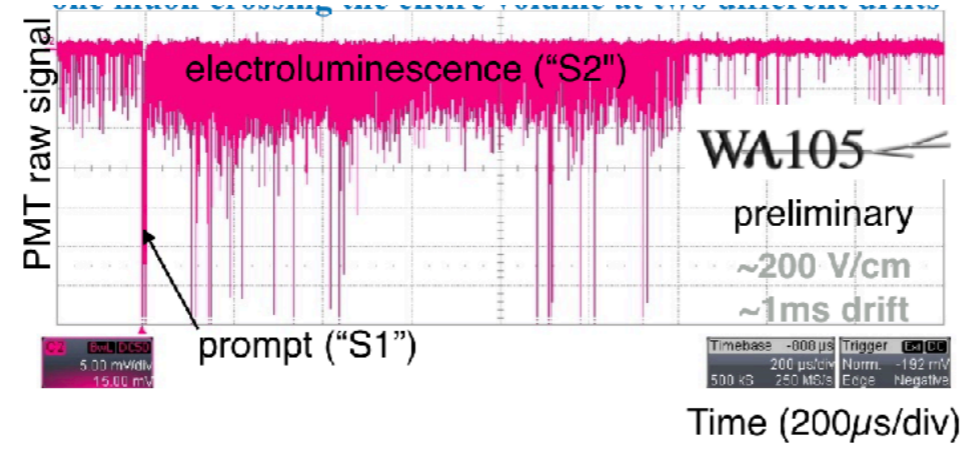
**2016 - Detector installation completed**



**Jan 2017 - Commissioning started**



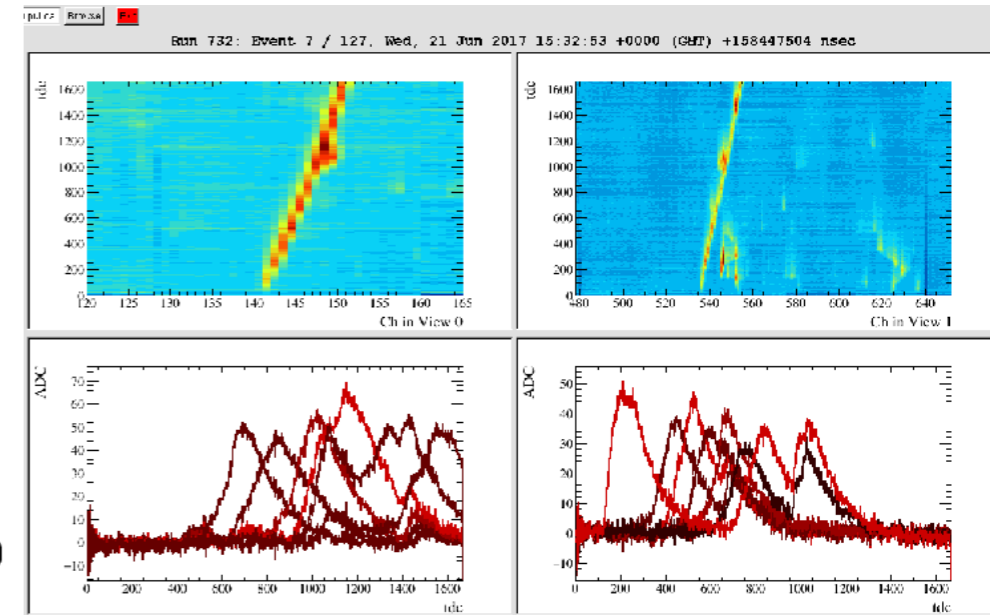
**Mar 2017 - Operation 'frozen' due to cryostat issues**

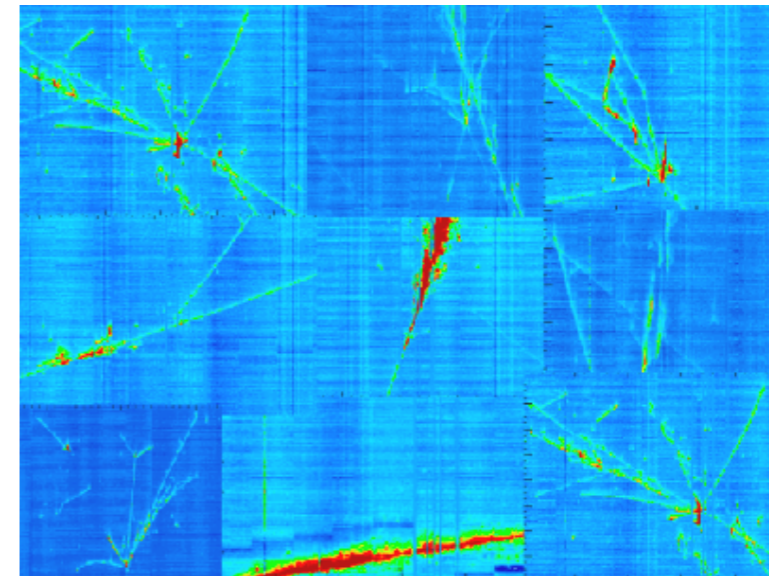
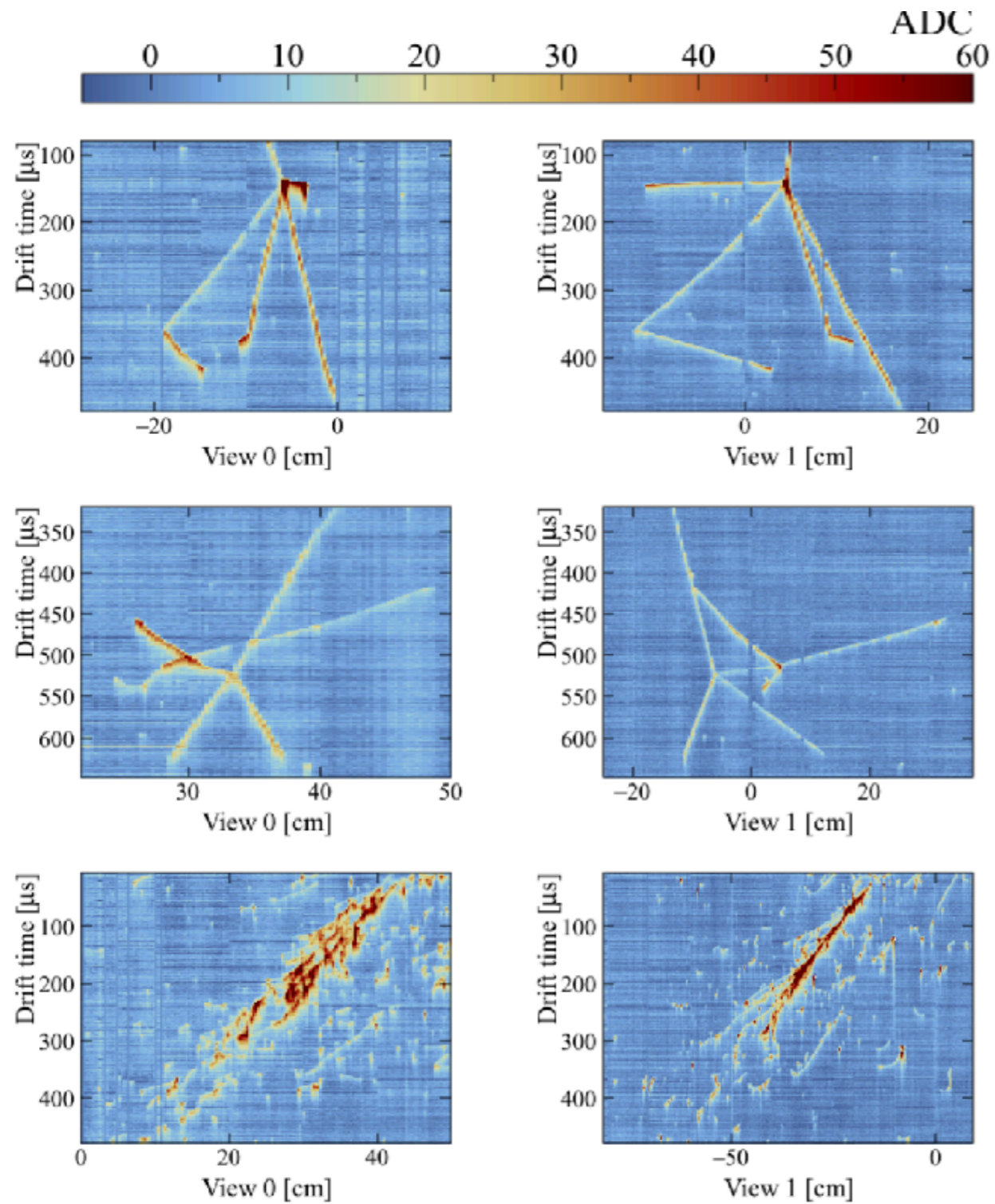


**June 12<sup>th</sup> - Recirculation started**

**June 15<sup>th</sup> - evidence of extraction from LAr to GAR**

**June 21<sup>st</sup> 2017 - First tracks observed**





**~400 k cosmic events recorded.**

hadronic and EM showers from cosmic rays recorded in the 3x1x1

## Journal of Instrumentation

### OPEN ACCESS

## A 4 tonne demonstrator for large-scale dual-phase liquid argon time projection chambers

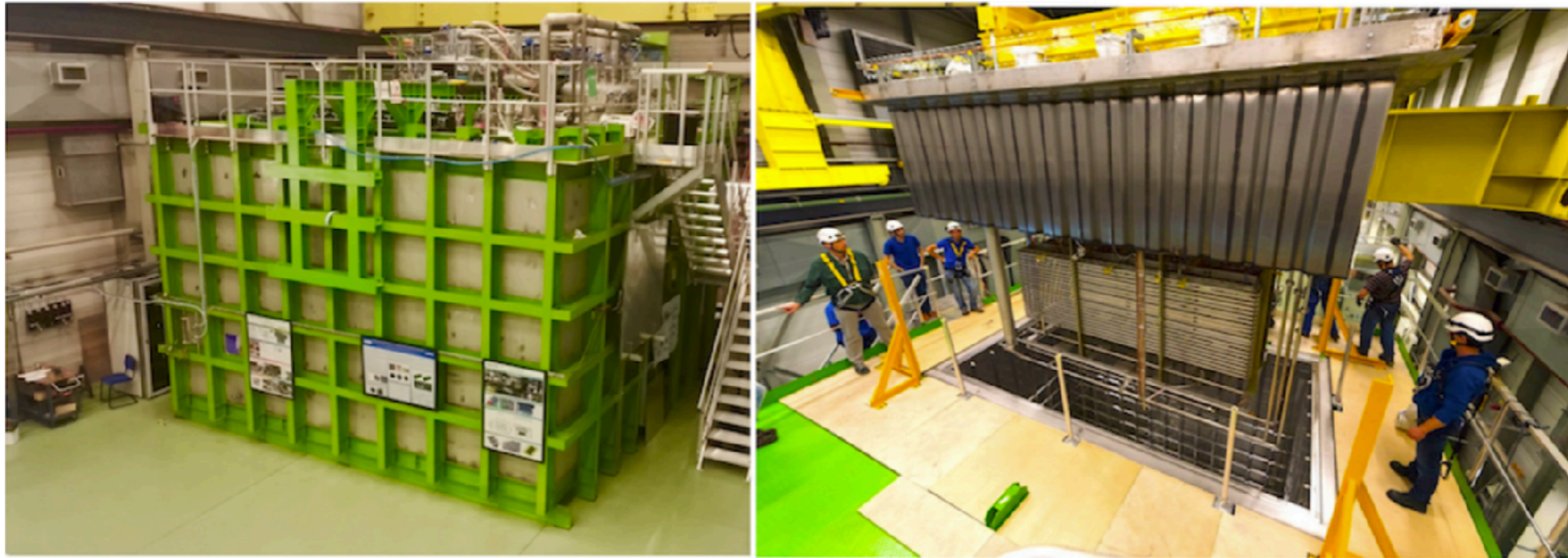
B. Aimard<sup>i</sup>, Ch. Alt<sup>a</sup>, J. Asaadi<sup>i</sup>, M. Auger<sup>b</sup>, V. Aushev<sup>v</sup>, D. Autiero<sup>c</sup>, M.M. Badoi<sup>r</sup>, A. Balaceanu<sup>r</sup>, G. Balik<sup>i</sup>, L. Balleyguier<sup>c</sup> [+Show full author list](#)

Published 6 November 2018 • © 2018 CERN

[Journal of Instrumentation, Volume 13, November 2018](#)

- Submitted to Arxiv in June 2018, published in JINST November 2018
- [Detailed summary of the detector design and performance in 60 page article.](#)

1	<b>Contents</b>	
2	<b>1 Introduction</b>	<b>3</b>
3	<b>2 Overview of the experimental apparatus</b>	<b>4</b>
4	2.1 Experimental setup . . . . .	4
5	2.2 Key concepts of dual-phase readout . . . . .	6
6	2.3 Technological milestones . . . . .	10
7	<b>3 Cryostat and cryogenic system</b>	<b>11</b>
8	3.1 The cryostat . . . . .	11
9	3.2 The cryogenic and argon purification systems . . . . .	14
10	3.2.1 Gas argon piston purge, cooling down and filling . . . . .	14
11	3.2.2 Boil-off compensation and argon purification . . . . .	16
12	<b>4 Description of the detector</b>	<b>17</b>
13	4.1 TPC drift cage and drift field high voltage . . . . .	17
14	4.2 Charge readout plane . . . . .	19
15	4.2.1 LEMs and anodes: design and quality assurance . . . . .	19
16	4.2.2 Mechanical frame assembly and cryogenic tests . . . . .	22
17	4.2.3 Electrical connections and properties, charge injection . . . . .	24
18	4.3 Photon detection system . . . . .	26
19	<b>5 Ancillary instrumentation and detector control system</b>	<b>28</b>
20	5.1 Pressure and temperature monitoring . . . . .	30
21	5.2 Liquid argon level monitoring and CRP motorisation systems . . . . .	30
22	5.3 Cryogenic cameras . . . . .	32
23	5.4 CRP high voltage system . . . . .	33
24	5.5 Detector slow control back-end . . . . .	34
25	<b>6 Detector readout, data acquisition and processing</b>	<b>36</b>
26	6.1 Charge readout overview . . . . .	36
27	6.2 Charge signal feedthroughs . . . . .	37
28	6.3 Analogue front-end cards . . . . .	39
29	6.4 Digital electronics, timing, and data acquisition . . . . .	40
30	6.5 Event triggering . . . . .	43
31	6.6 Online data processing and storage . . . . .	44
32	6.7 Grounding and noise in charge readout chain . . . . .	46
33	<b>7 Detector performance</b>	<b>47</b>
34	7.1 Cryogenic system performance and stability of the liquid argon surface . . . . .	47
35	7.2 Observation of prompt scintillation and electroluminescence . . . . .	48
36	7.3 TPC charge readout and operational feedback . . . . .	51
37	7.3.1 Electric field settings . . . . .	51
38	7.3.2 First look at data: cosmic muons with gain . . . . .	54
39	<b>8 Conclusions</b>	<b>59</b>



- Performance of the cryogenic system and of the 23m<sup>3</sup> membrane cryostat.
- Extraction of the ionisation charge over an area of 3m<sup>2</sup>.
- Amplification in pure argon vapour by a combined operation of multiple 50 × 50 cm<sup>2</sup> LEMs
- Readout of the signal on two collection planes with strips of up to 3 m length and performance of analogue front-end electronics.
- Detection of prompt and secondary scintillation.



The goal of the cryostat and cryogenic system is to ensure during extended operating periods:

## **1. stable thermodynamic conditions**

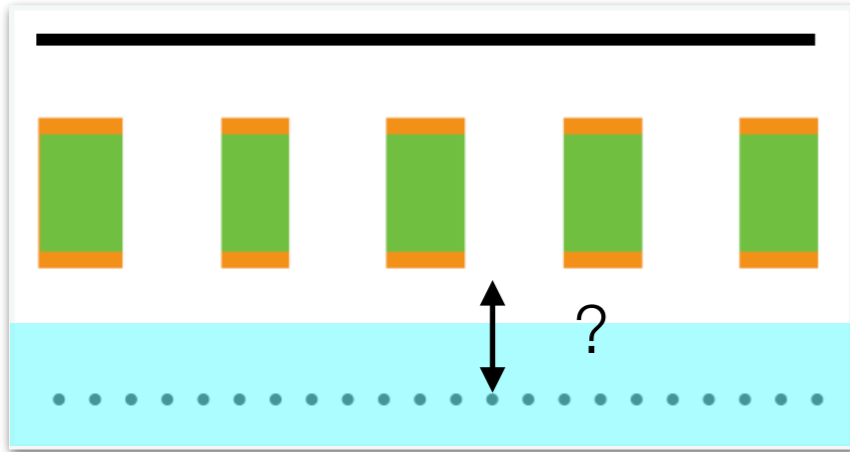
- Uniform and stable gas argon density near 1 Atm and 90 K completely isolated from outside  
P,T fluctuations
- operation of Front End electronics near 110 K
- compensate the heat input of cryostat by active cooling

## **2. stable liquid level during liquid recirculation**

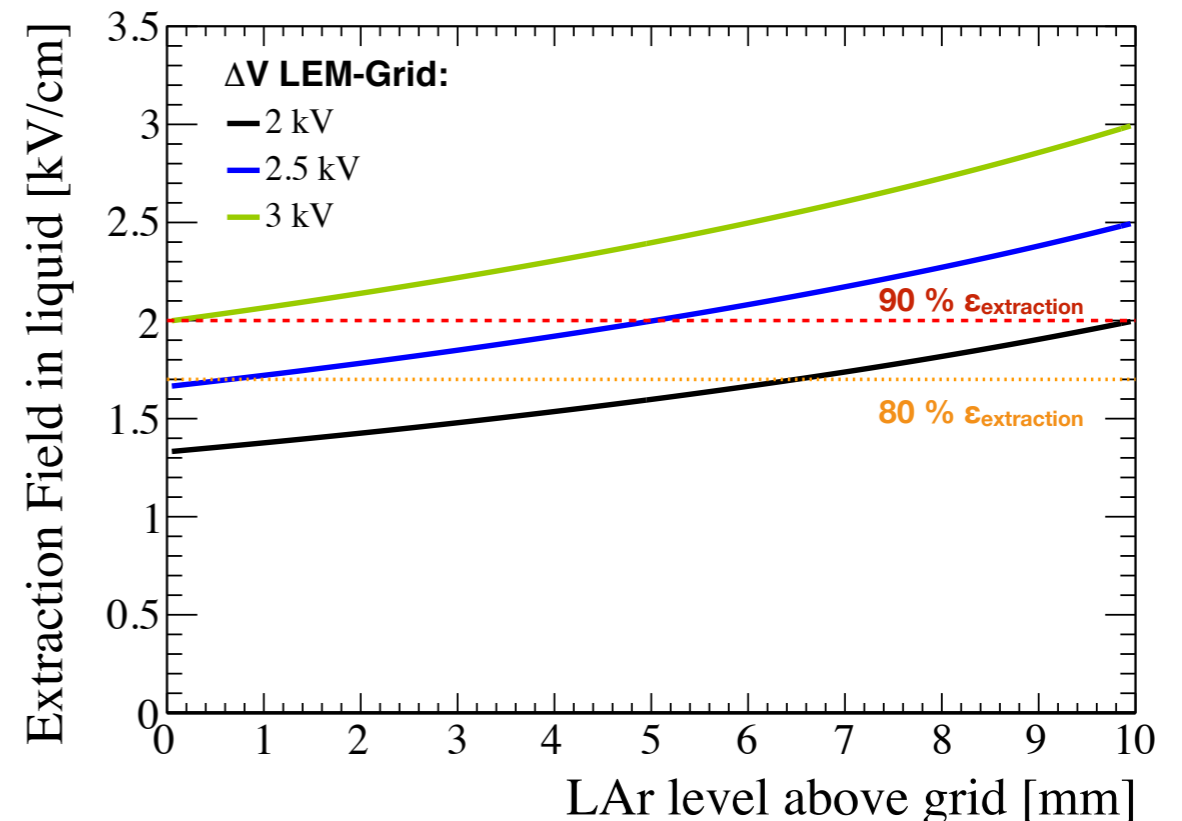
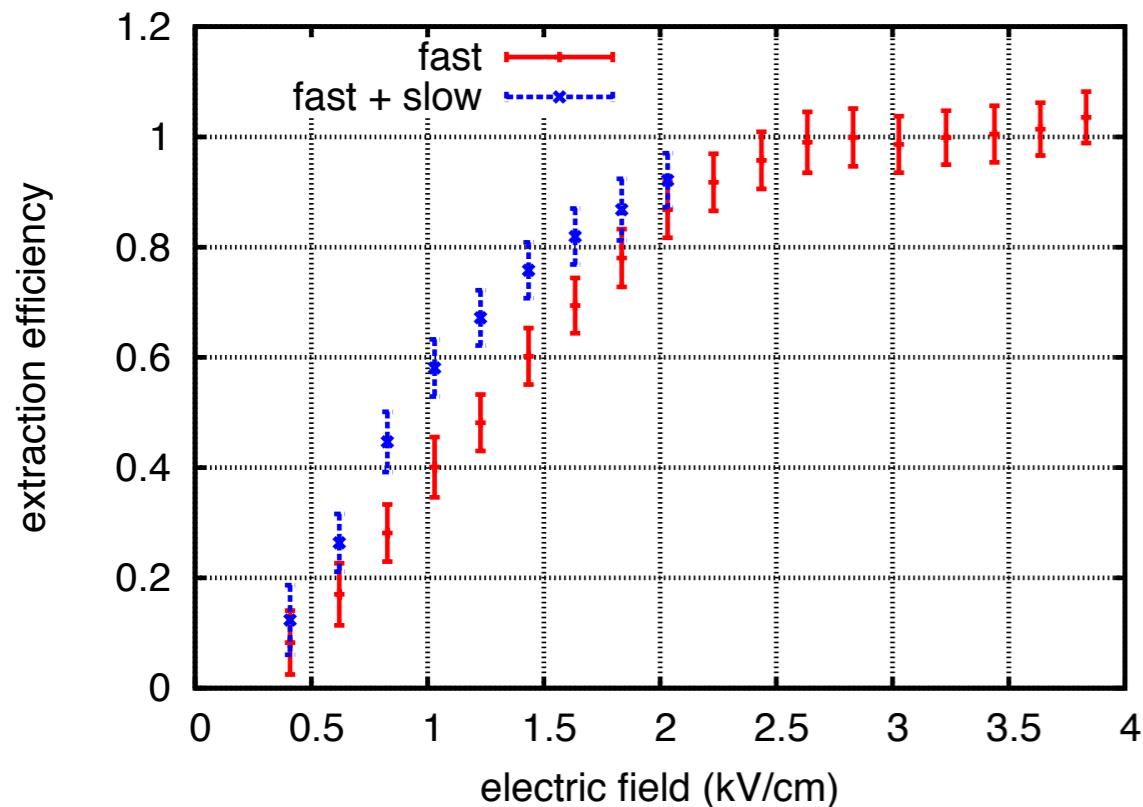
- Avoid slow fluctuations of level which might be induced by regulation of cryo system
- avoid fast fluctuations (=waves) which might be induce from local heat inputs (i.e bubbling) and defect in cryostat insulation.

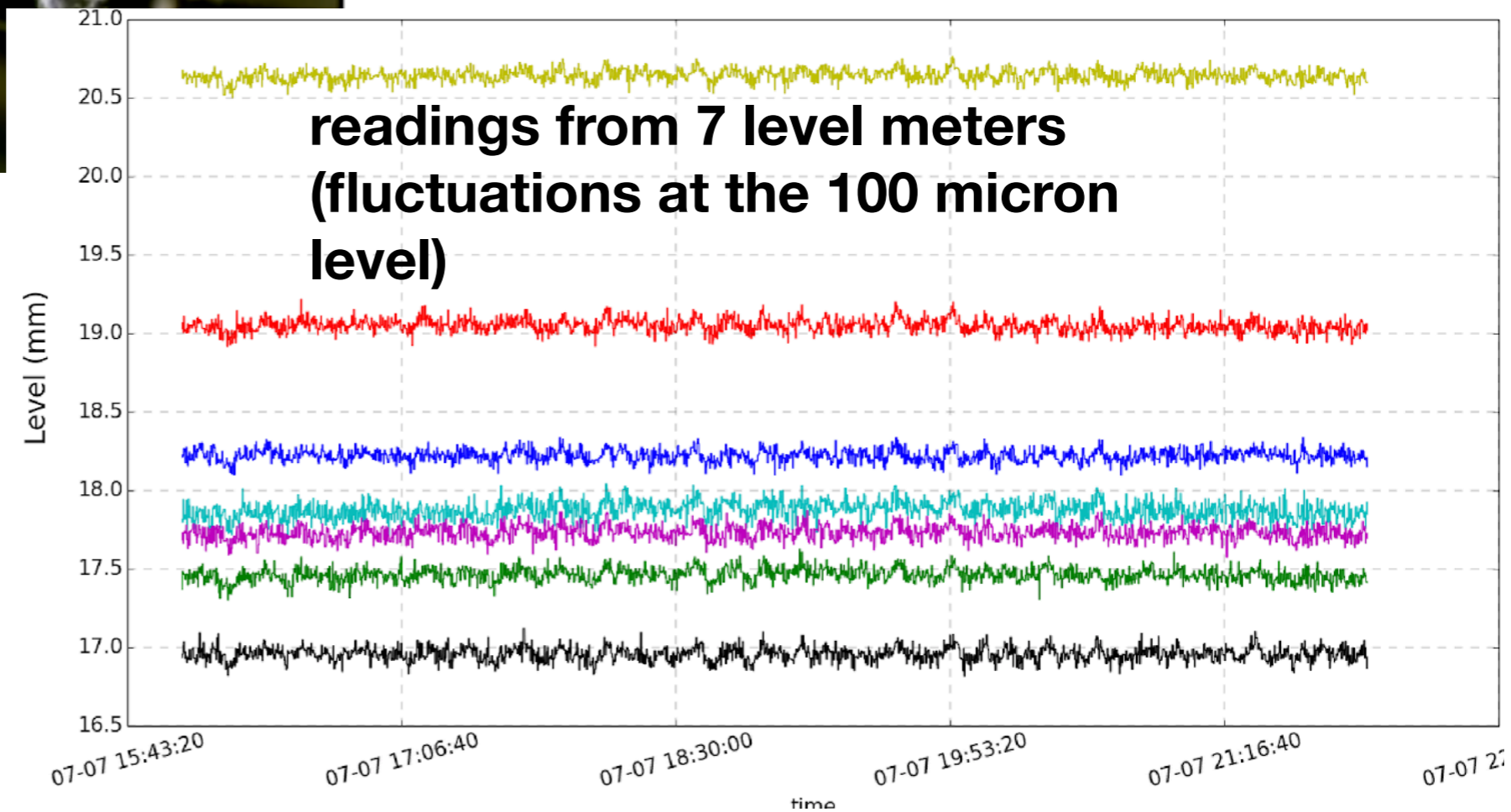
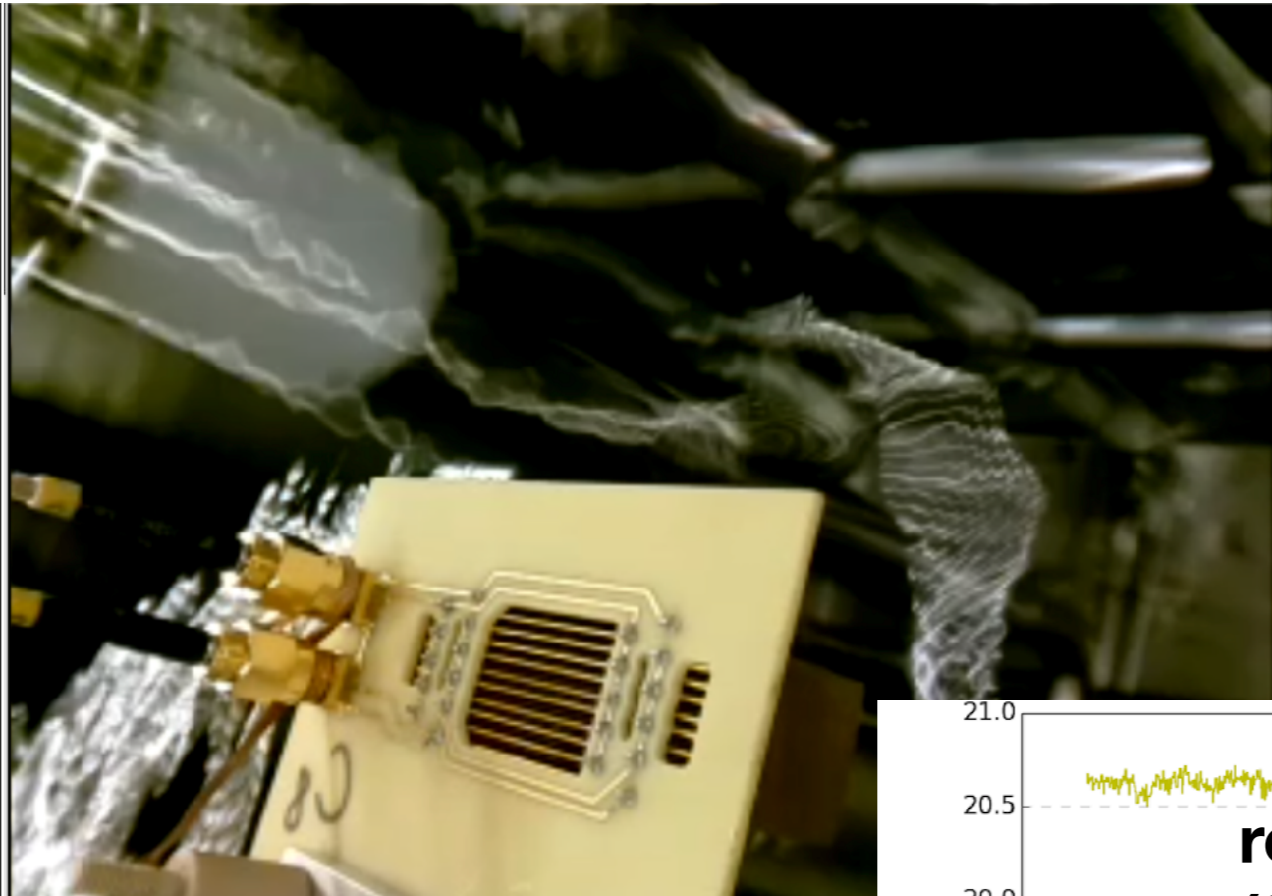
## **3. high liquid argon purity:**

- better than 3 ms drift or less than 100 ppt O<sub>2</sub> equivalent impurities

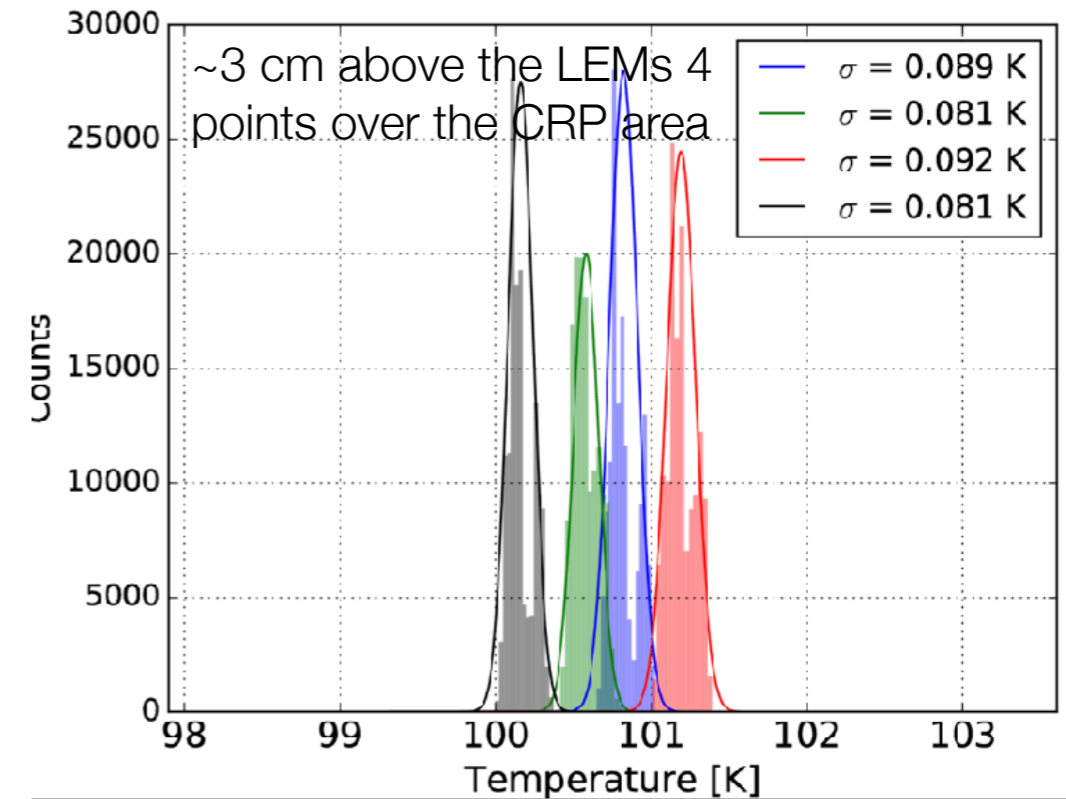


- an important point on requirement of level position:
- for a given  $\Delta V_{\text{LEM-grid}}$  the extraction *field* depends on the position of the LAr level.
  - At sufficiently large  $\Delta V_{\text{LEM-grid}}$  ( $> \sim 2.5$  kV) the extraction *efficiency* (hence the gain) is near maximal and therefore almost independent of the liquid level.
  - The boundary conditions are (of course) that the liquid should not touch the LEMs and the grid stays immersed.
  - ->LAr level and CRP alignment to the LAr level within 1 mm and monitoring within 100 microns

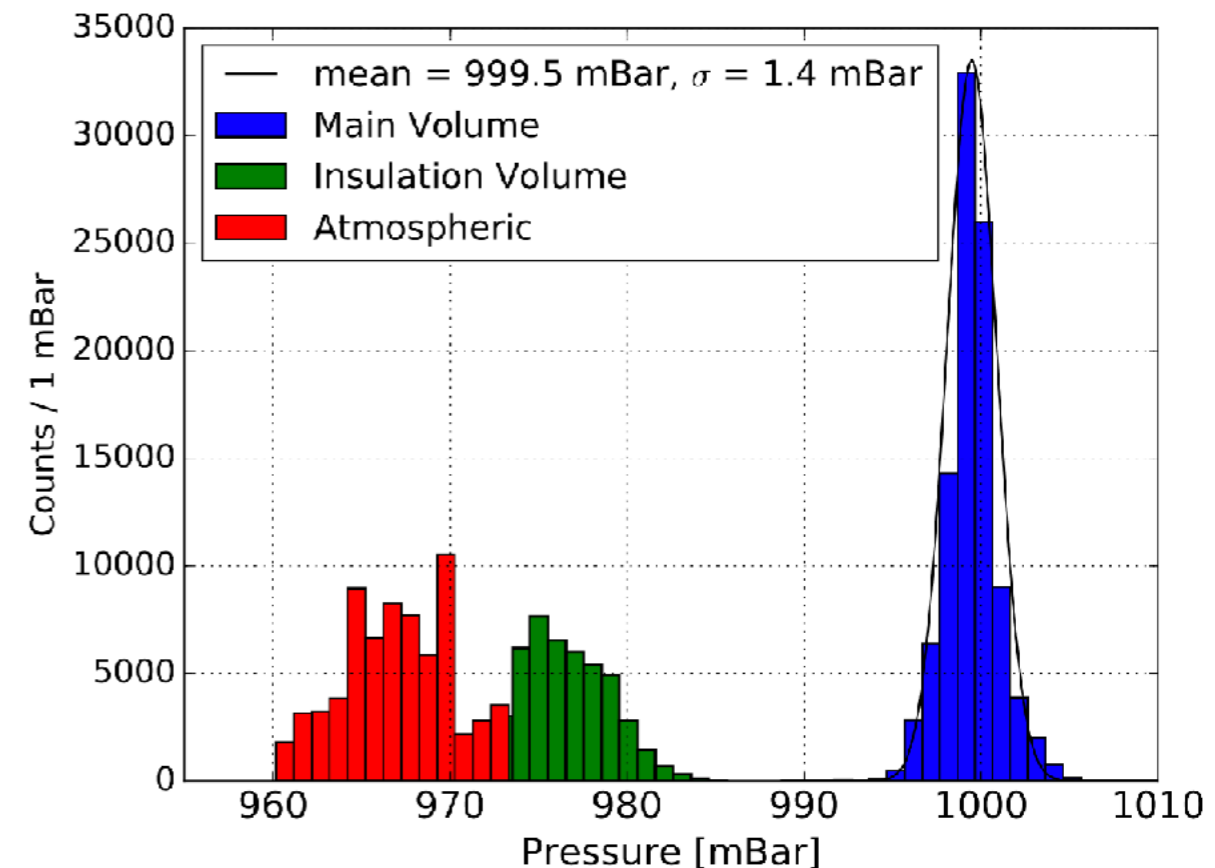


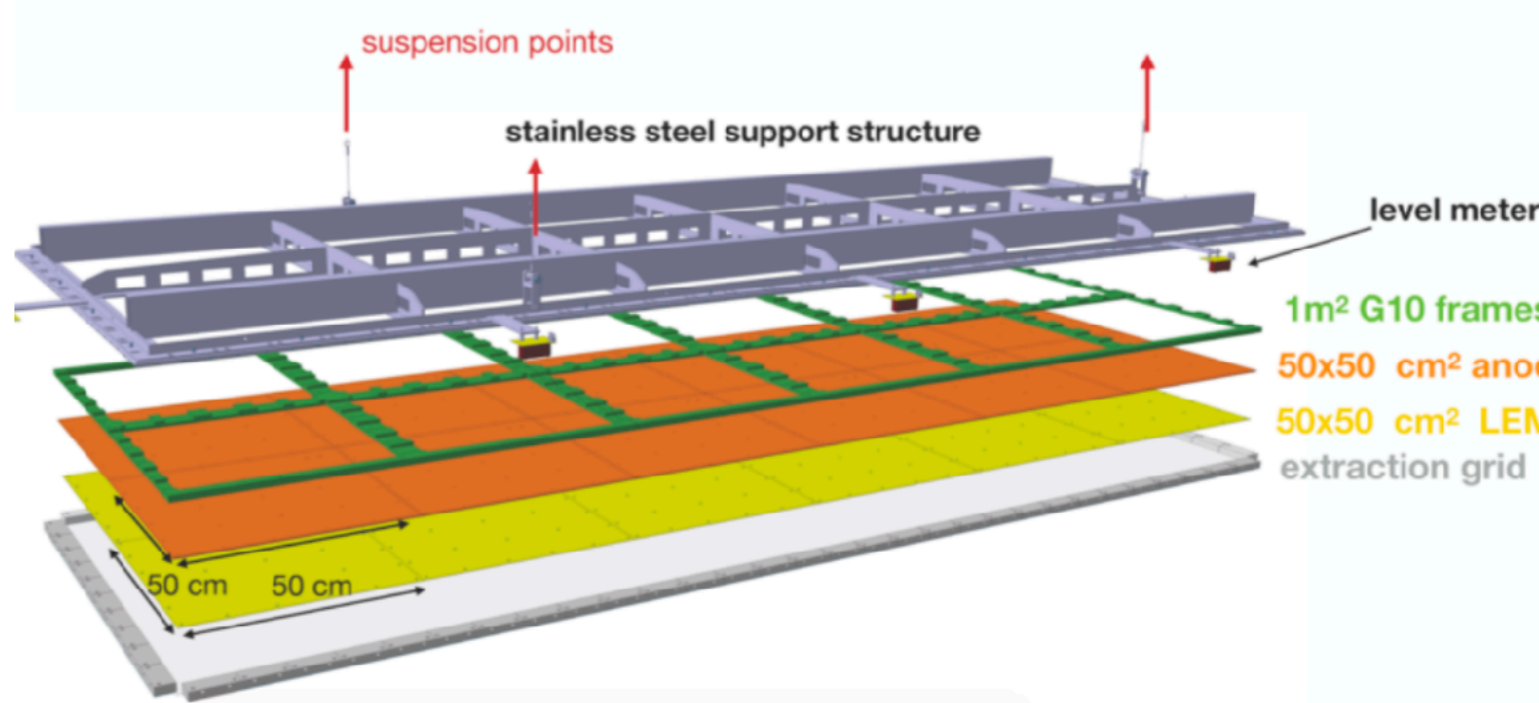
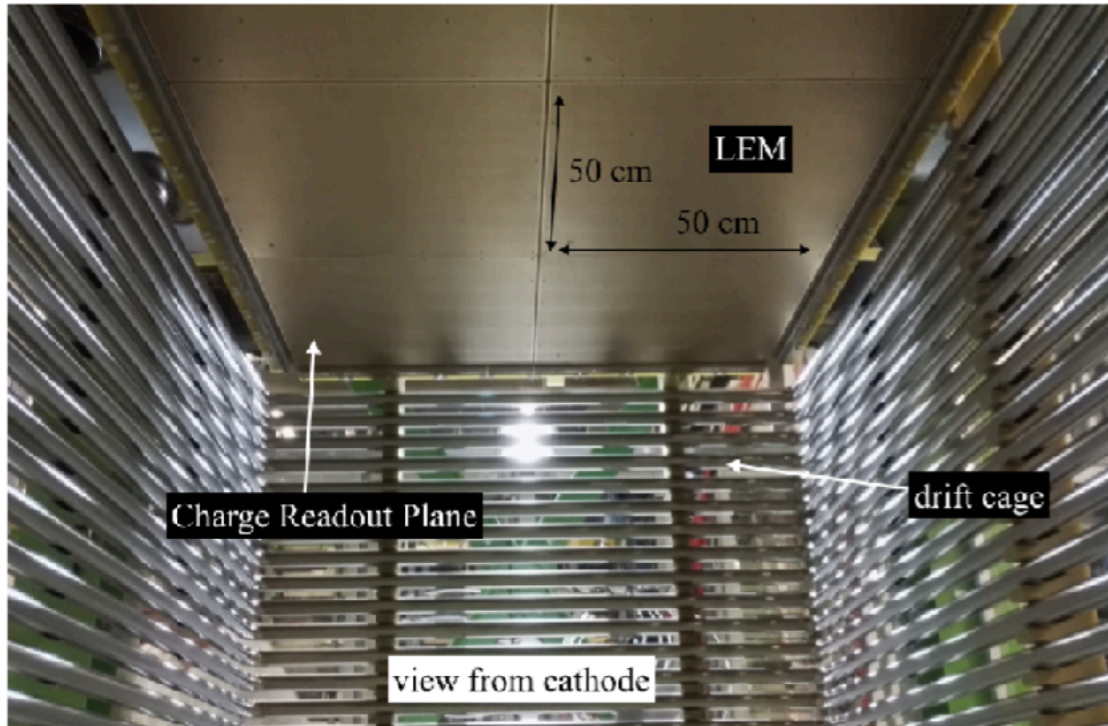


- Temperature is uniform across the CRP.
- measured gradient near LAr surface is uniform at  $\sim 2$  K/cm



- Pressure is stable at  $999 \pm 1$  mbar decoupled from external pressure variations





Precisely machined frame that allows to position the extraction-grid, LEMs and anodes with well determined inter-stage distances.

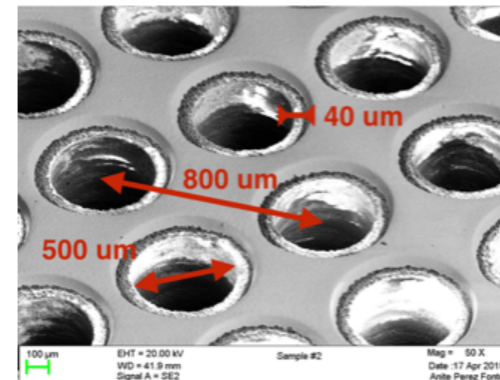
The frame is remotely adjustable to the liquid argon level with a precision of around 100 microns

Demonstrate:

- ➔ collective operation with gain of twelve LEMs arranged side by side
- ➔ extraction on 3m<sup>2</sup> area and charge readout on 3m long strips

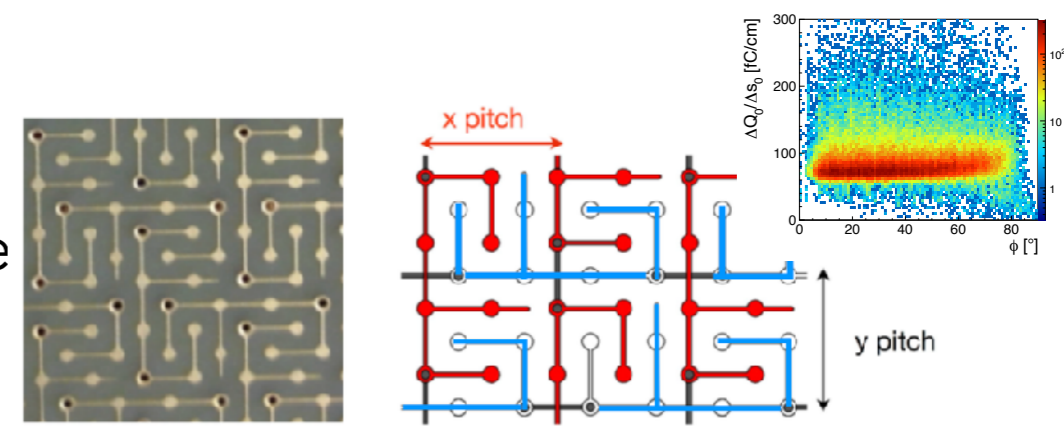
- **LEMs and anode**

- large area LEMs (50x50 cm<sup>2</sup>) o(150) holes per cm<sup>2</sup>.  
Intrinsic geometrical parameters (rim, hole, pitch)  
optimised from test on smaller devices.



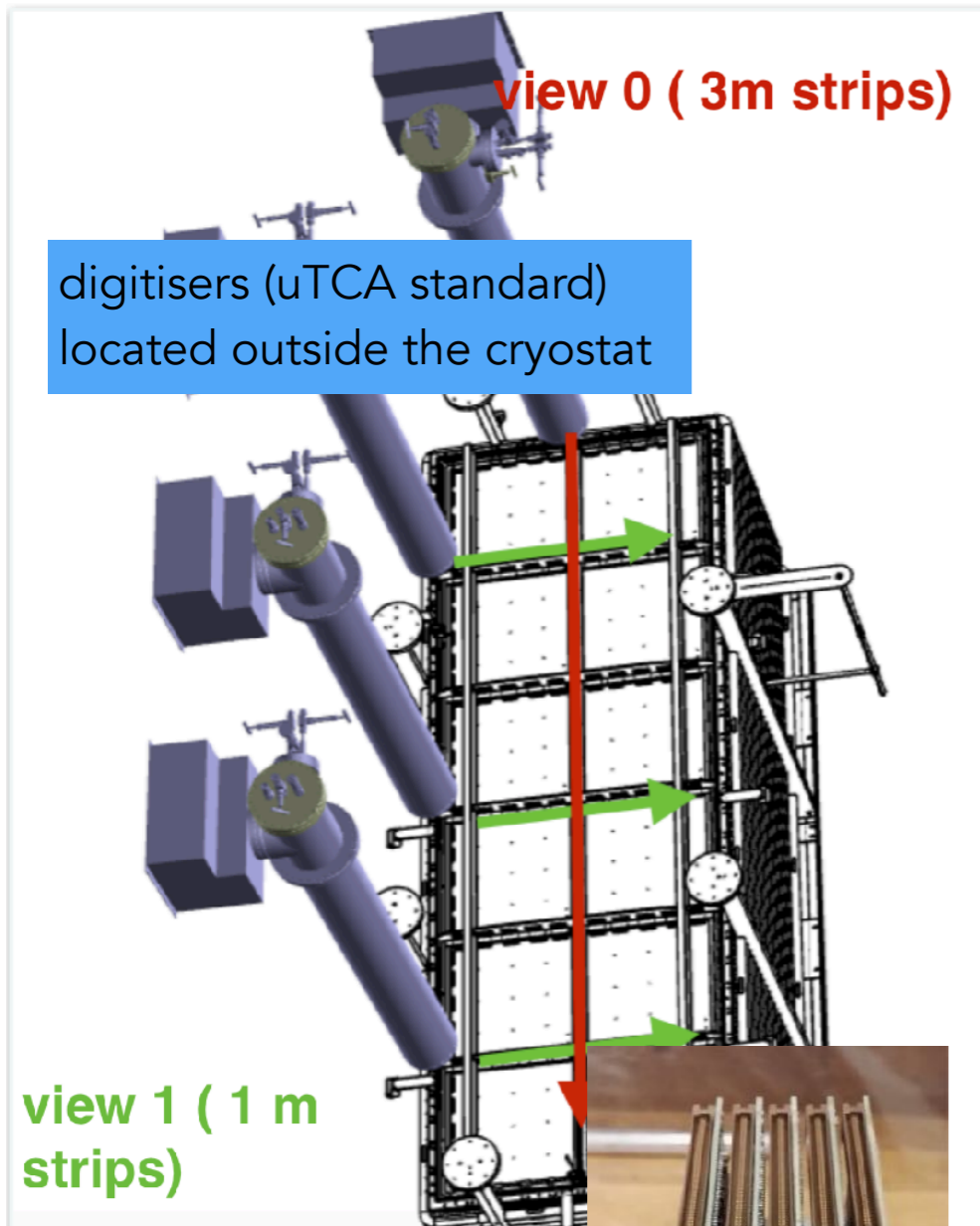
literature  
NIM A617 (2010) p188-192  
NIM A641 (2011) p 48-57  
JINST 7 (2012) P08026  
JINST 8 (2013) P04012  
JINST 9 (2014) P03017  
JINST 10 (2015) P03017

- Two view collection anodes with fine 3 mm segmentation: designed to provide identical charge sharing between both views with strip capacitance per unit length as low as 150 pF/m



- **CRP Mechanical behaviour at cold**: open bath LN2 test (shock cooling) with mechanical deformations monitored by photogrammetry





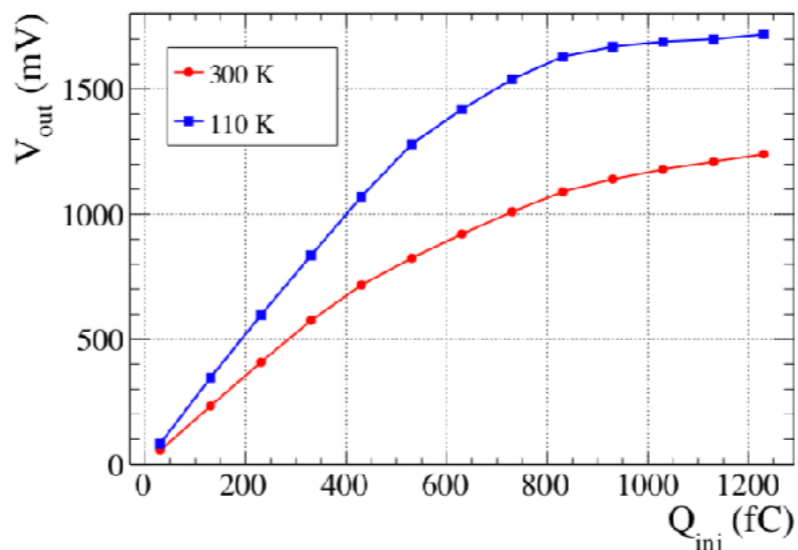
digitisers (uTCA standard)  
located outside the cryostat

view 1 (1 m strips)

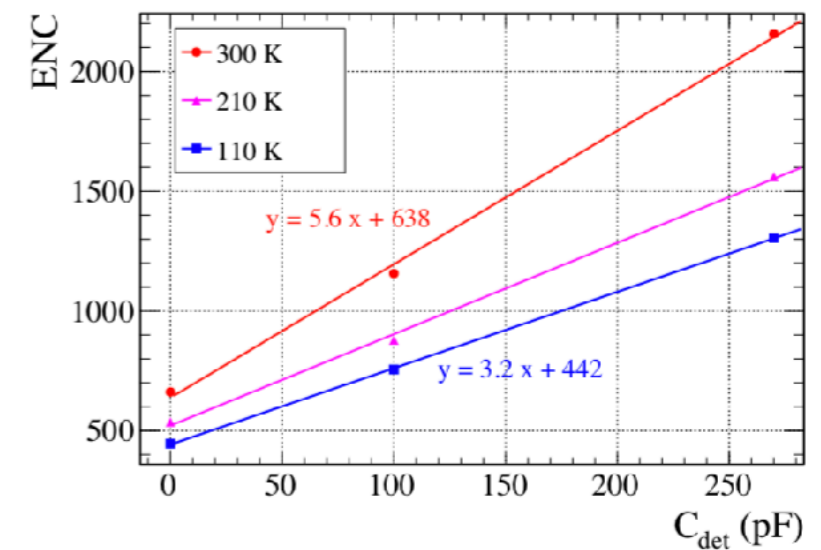
FE ASIC amplifiers located inside custom made "signal" feedthroughs isolated from main argon volume

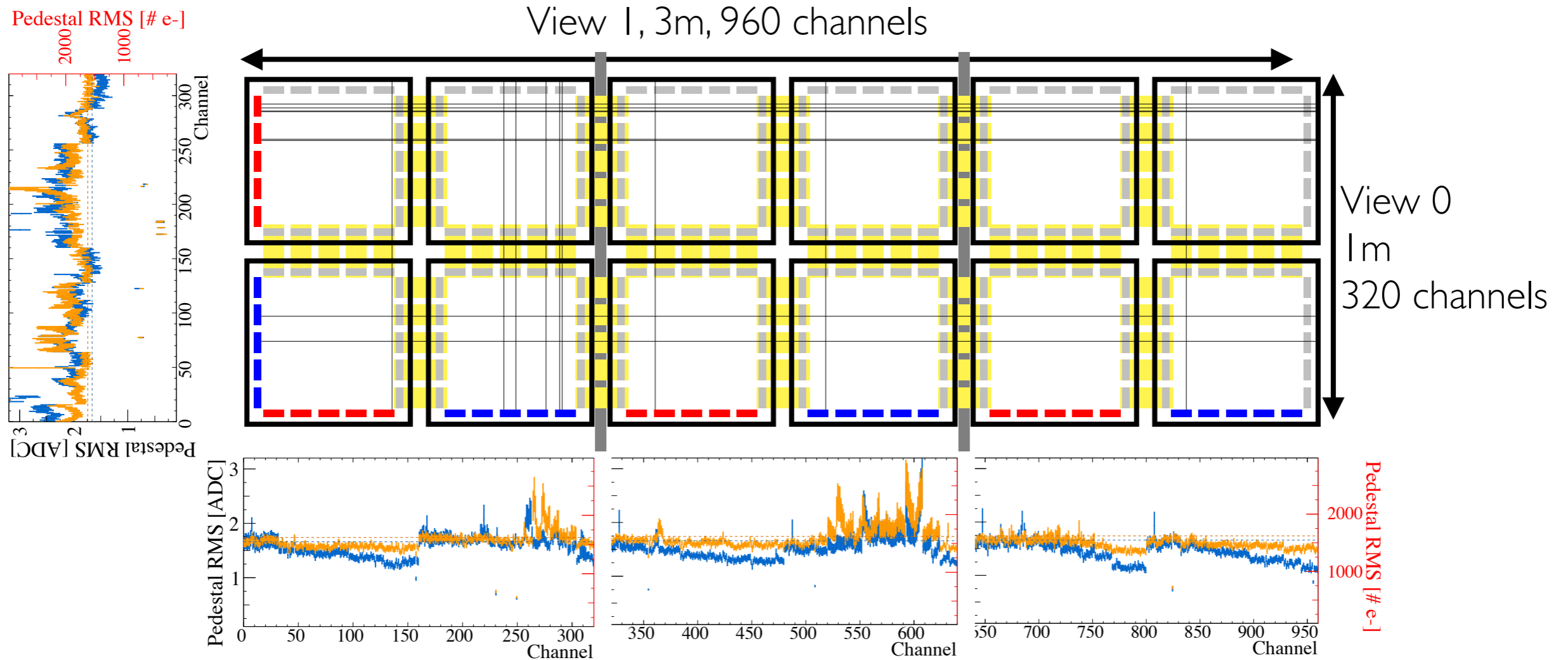
- DP detector design that allows:
- the operation of FE amplifiers at **cryogenic temperatures** (stable ~140 K as measured during 3x1x1 data taking)
  - the positioning of the FE amplifiers **close to the anodes**.
  - the **accessibility** of the FE cards at any time during detector operation for replacement or maintenance.

Double slope gain with dynamic range up to 1200 fC



Equivalent Noise charge vs detector capacitance





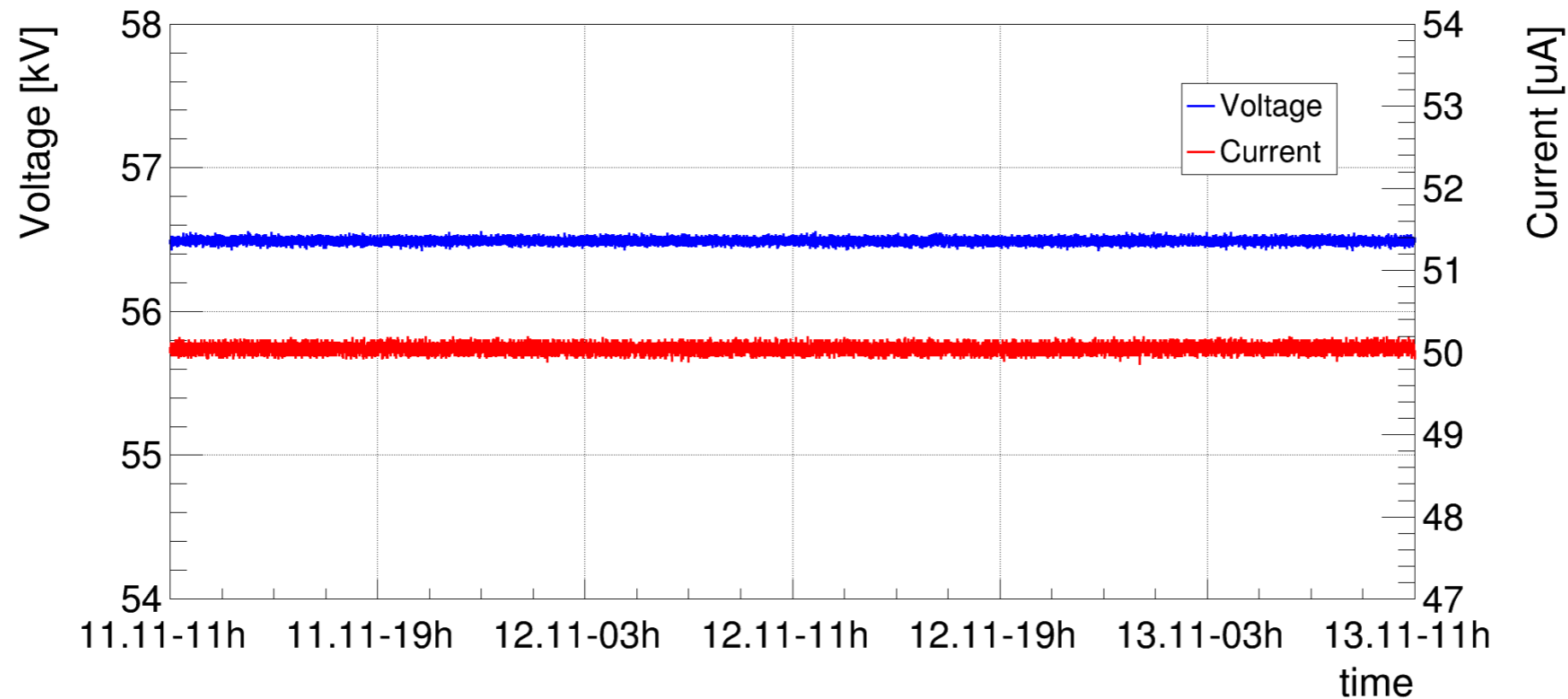
- Noise at cryogenic temperature stable at around 1550 e<sup>-</sup>
- M.I.P Signal on one channel expected around (infinite electron lifetime):
  - ~10 ke for effective gain 2 (S/N=10)
  - ~100 ke for effective gain 20 (S/N=100)

✓ Noise is below 2'000 electrons on 3 m long strips



Cathode

Heinzinger PNChp 100000 -neg, ethernet readout

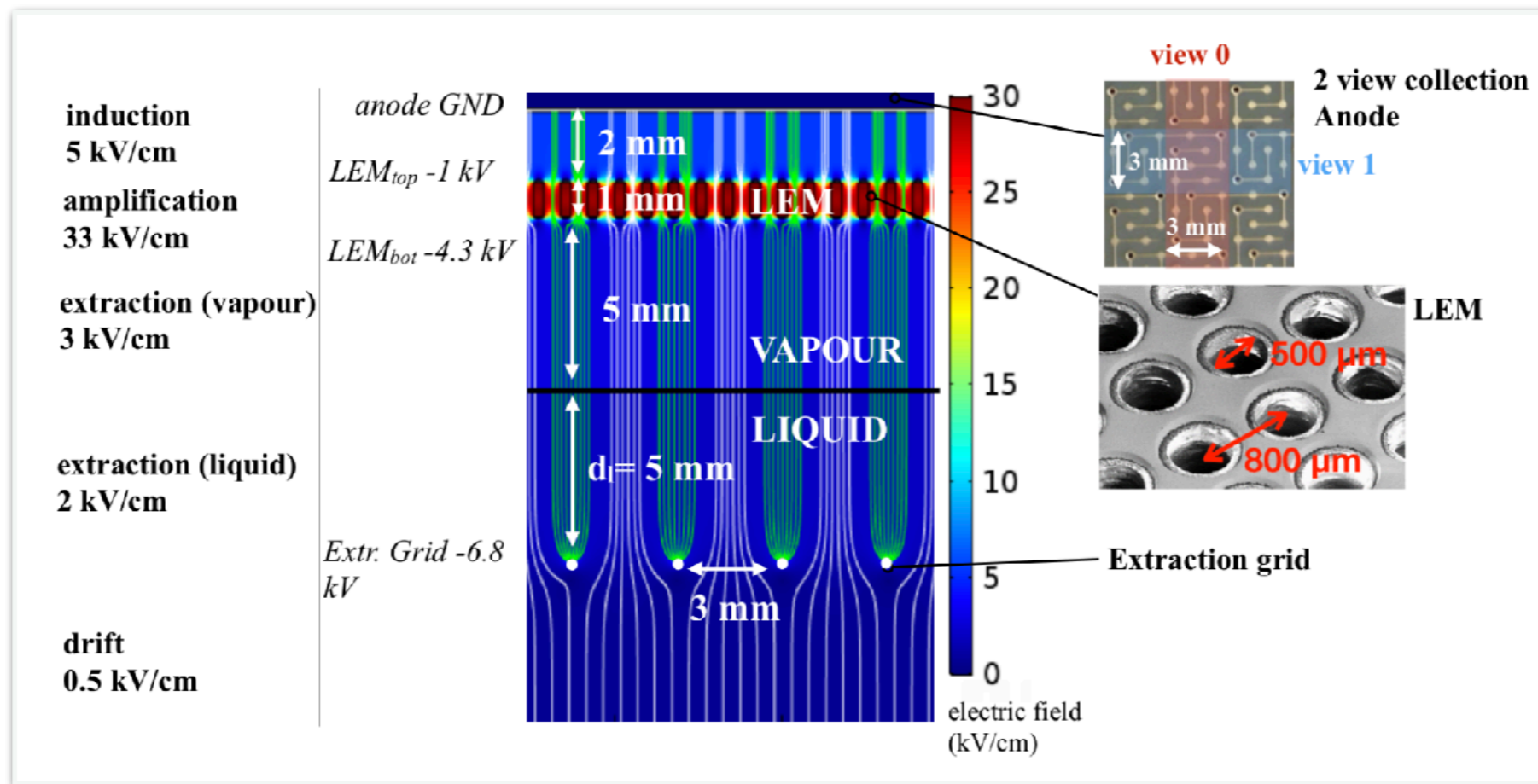


stable:

- current of  $50 \pm 0.08$  uA (as expected from the divider)
- voltage  $56.5 \pm 0.01$  kV

max voltages:

- on feedthrough alone: -300 kV [JINST 12 P03021 arXiv:1611.02085](#)
- on 3x1x1 cathode -65 kV for the entire duration of the data taking (no discharges, stable current)



- The extraction grid discharged at around -5 kV while the nominal voltage (for an effective gain of 20) is set to around -6.8 kV.
- Evidence (after dedicated tests and visual inspection) points to a group of 32 wires which were not correctly tensioned and a faulty HV contact.
- As a consequence we were not able to operate the detector at its full potential with the nominal voltages shown above.
- **Nevertheless we collected a large amount of good quality data at various field configurations.**

**Table 9.** Electric field settings explored during and data taking with the  $3 \times 1 \times 1 \text{ m}^3$  TPC (see text for more details). The values quoted as nominal correspond to  $G_{\text{eff}}^{\infty}$  of 20 as achieved in the dual-phase TPC with the  $10 \times 10 \text{ cm}^2$  readout area [15, 22].

Electric field (kV/cm)	Scanned range	Data taking settings	<i>Nominal</i>
Induction	1–5	1.5	5
Amplification <sup>33</sup>	23–31	28	33
Extraction (in liquid)	0.6–2.5	1.7	2
Drift	0.18–0.7	0.5	0.5

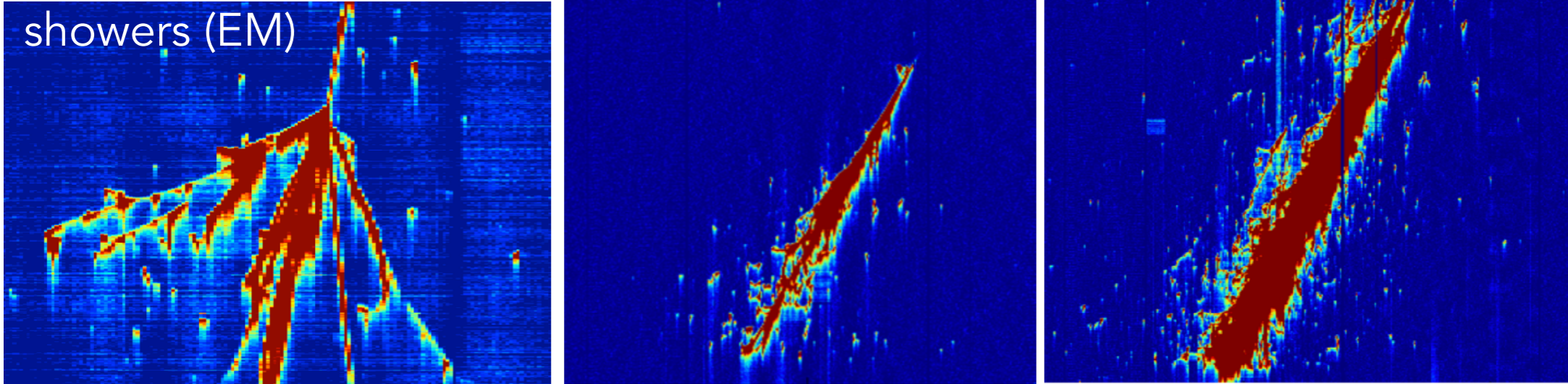
scanned ranges with max electric fields obtained independently on each element by reducing the other field values in order to be compatible with the overall limitation imposed by the grid HV.

Stable data taking settings. best compromise taking into account the limitation on the absolute grid HV

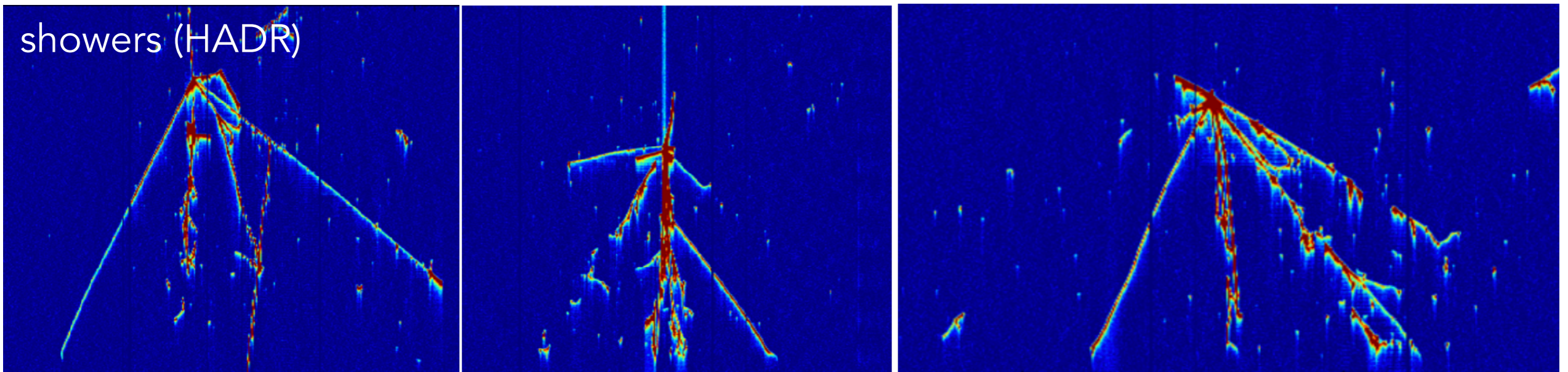
more than 400 k cosmic events collected

HV: data taking settings

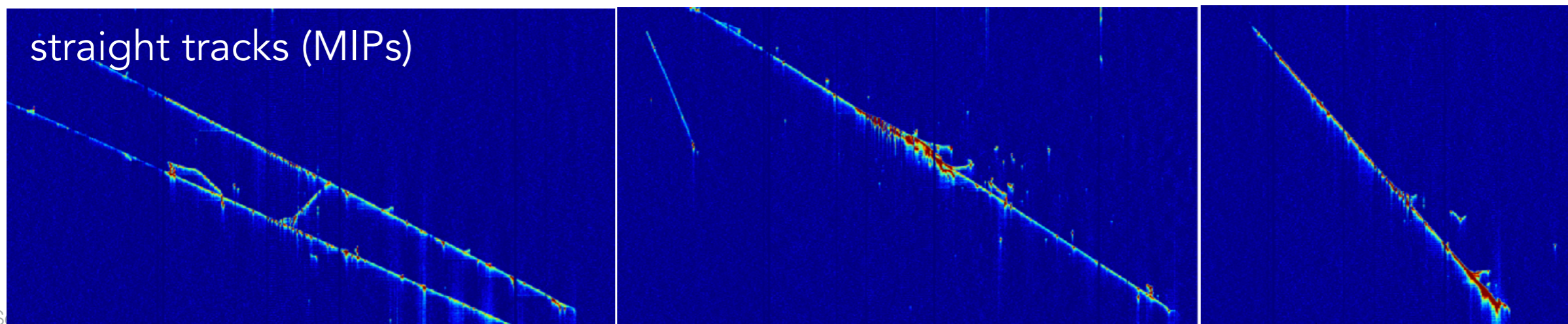
showers (EM)

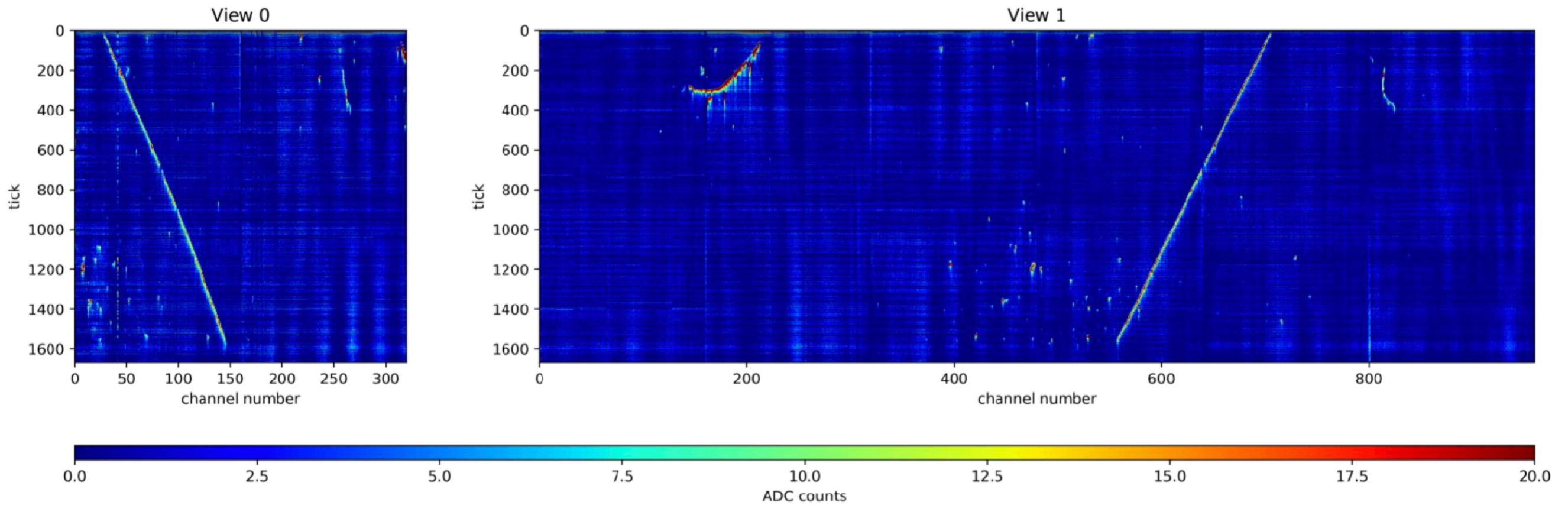


showers (HADR)



straight tracks (MIPs)





Crossing muons (MIPs): easy to reconstruct in 3D and deposits a known amount of charge of  $\sim 10$  fC/cm in liquid argon (at 500 V/cm and w/o attenuation due to drift)  
 $\Rightarrow$  characterise the TPC in terms of amplification (effective gain), LAr purity, charge sharing between views, ..

The signal measured on one view

charge sharing between views  
**50% charge sharing**

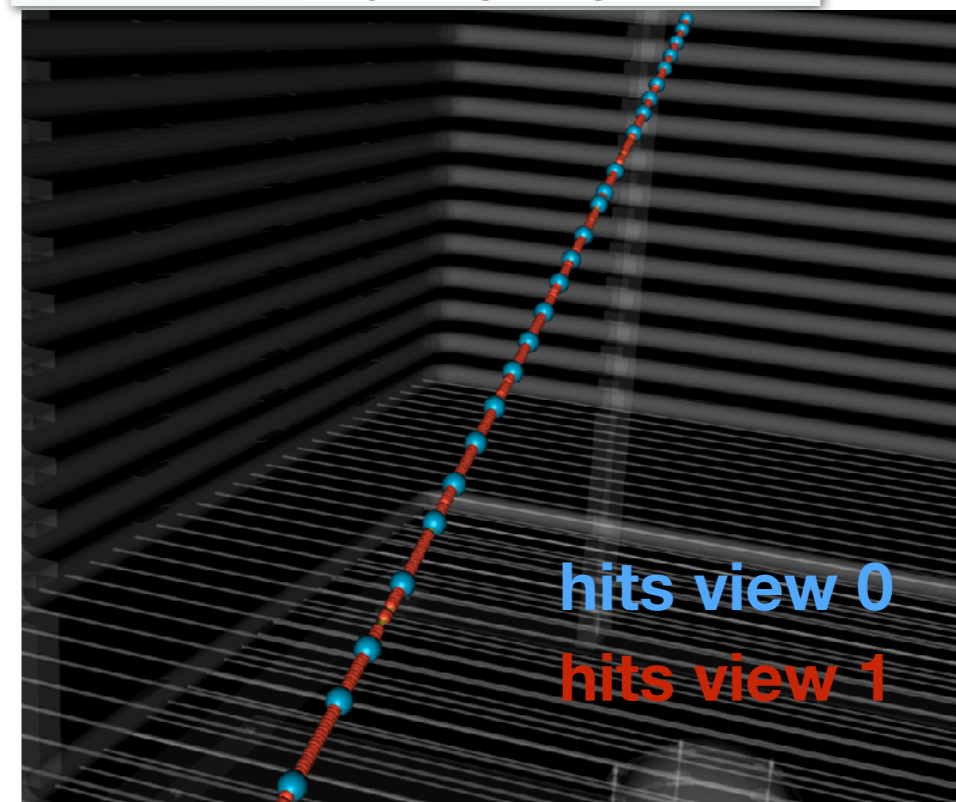
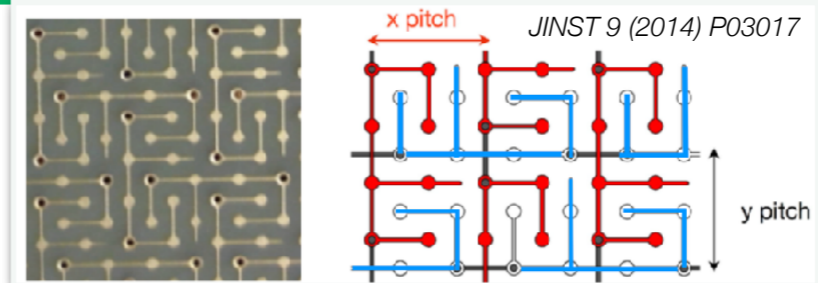
**effective gain**  
**goal 20**

**10 fC/cm** (at 500 V/cm drift)

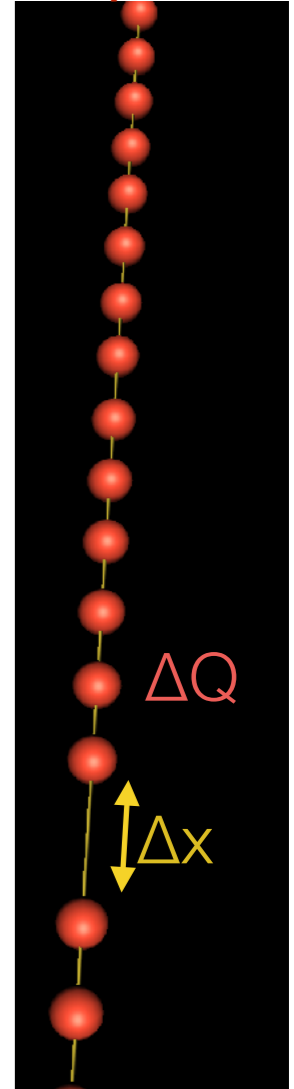
$$\left\langle \frac{dQ}{ds} \right\rangle_{view_i} = F_{share}(view_i) \times \epsilon_{extraction} \times G_{LEM} \times \epsilon_{induction} \times \left\langle \frac{dQ}{ds} \right\rangle_{MIP}$$

anode requirements:

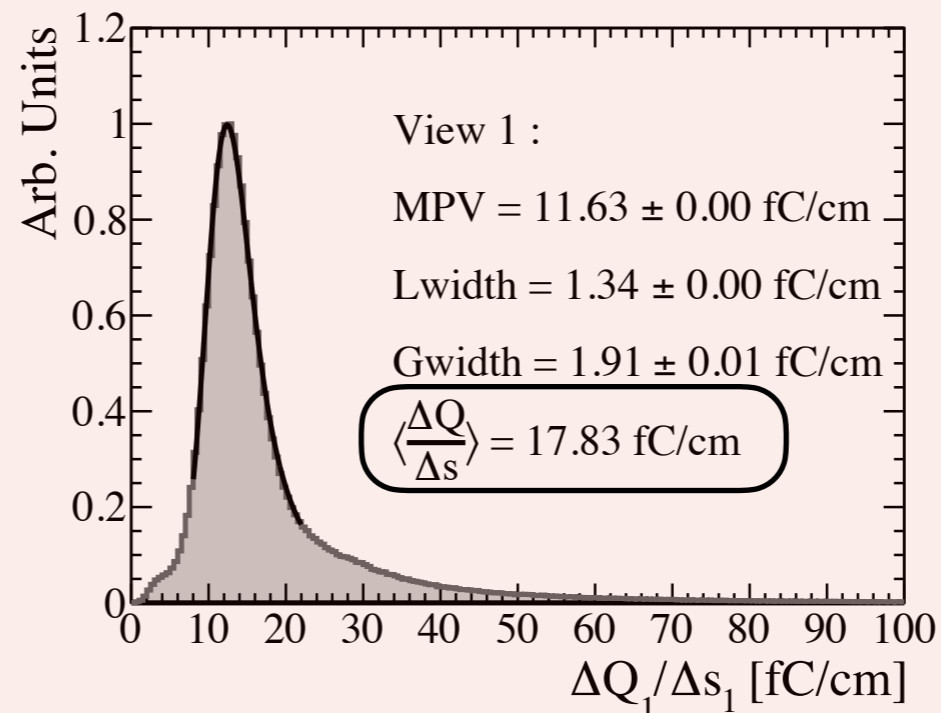
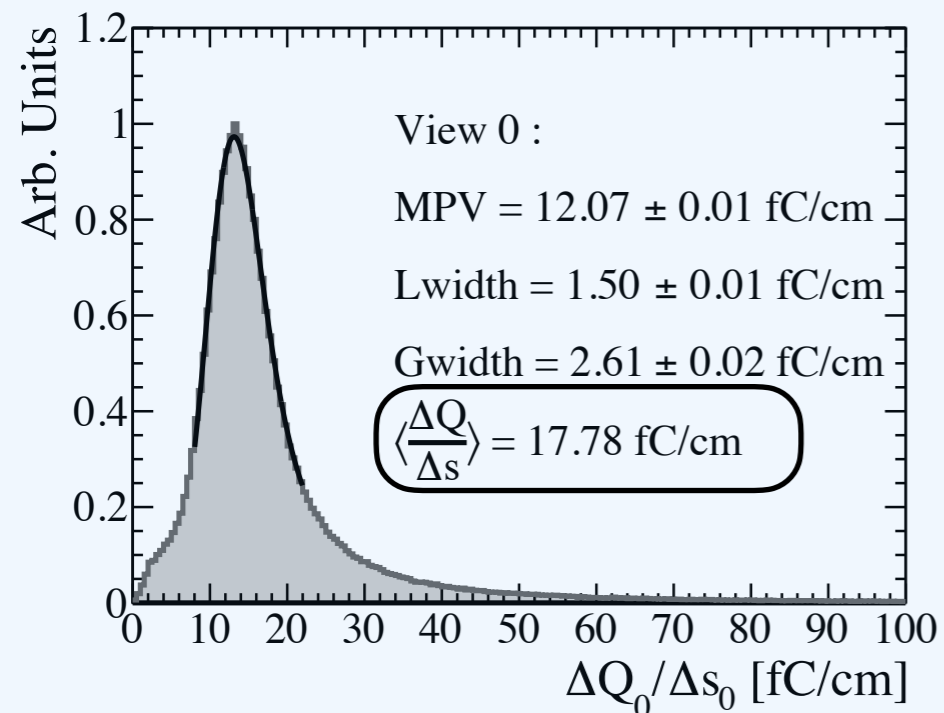
- low capacitance per unit length (<2000 e-noise equivalent)
  - 50:50 charge sharing between the strips.
- Tested at the cm strip scale (JINST 9 (2014) P03017)  
**50:50 charge sharing demonstrated here on 3x1 m2 strips**



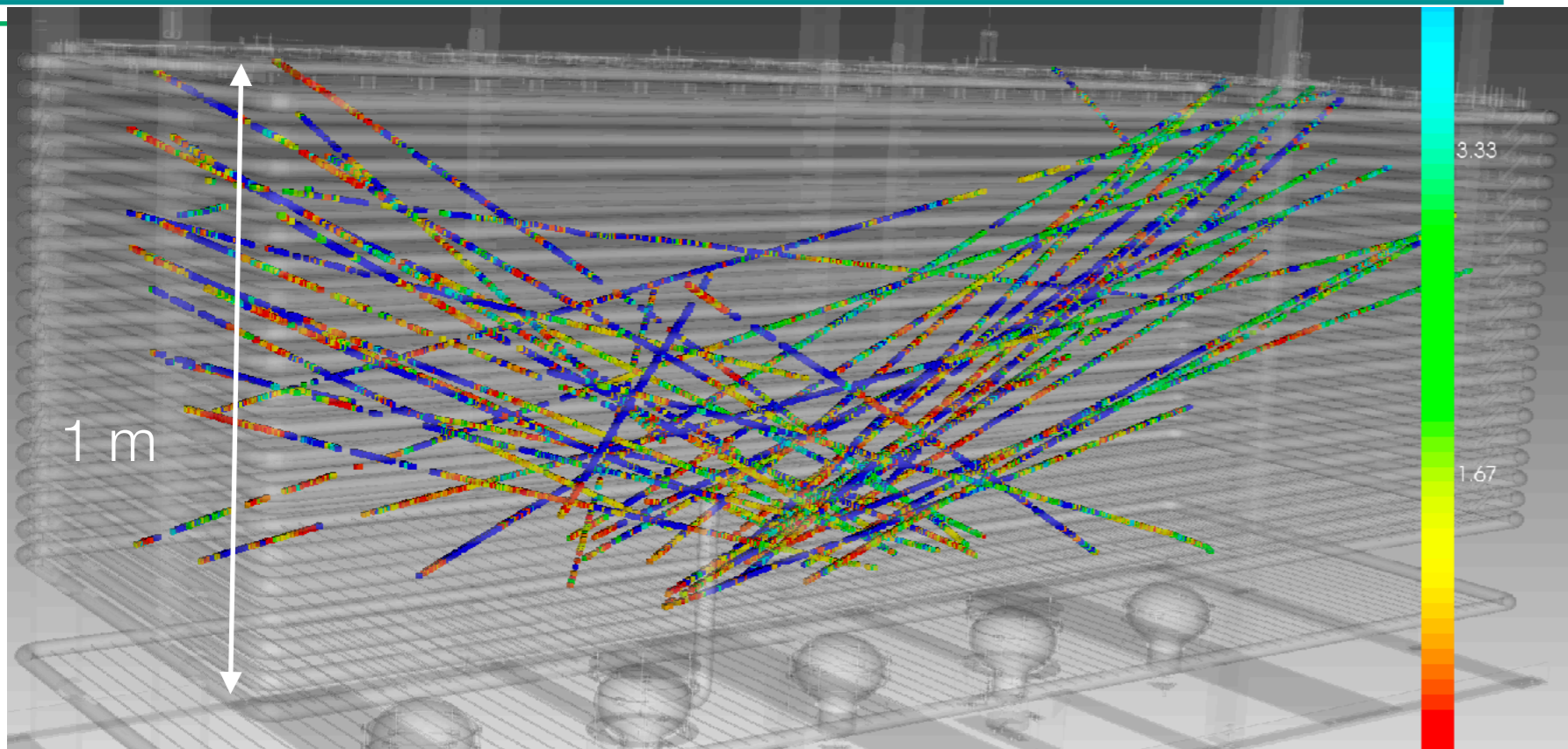
example hits view 0



From 3D reconstructed tracks:  
 calculate the  $\Delta Q/\Delta x$  per view



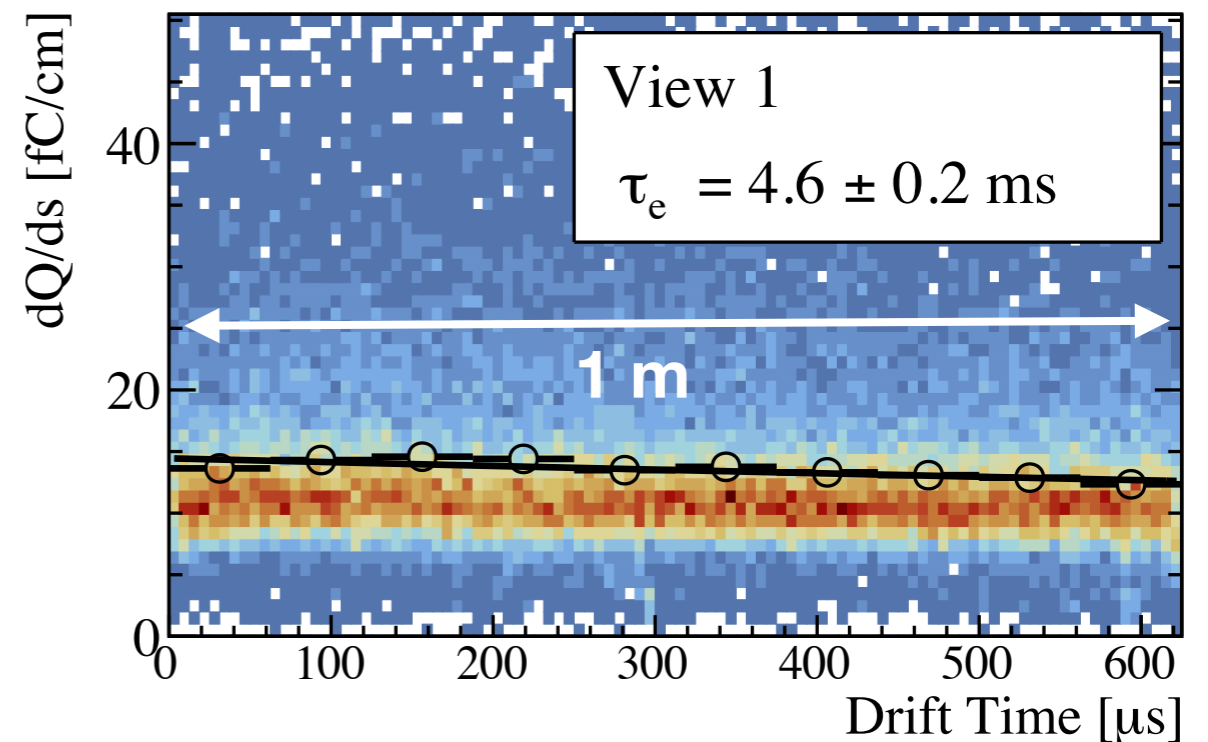
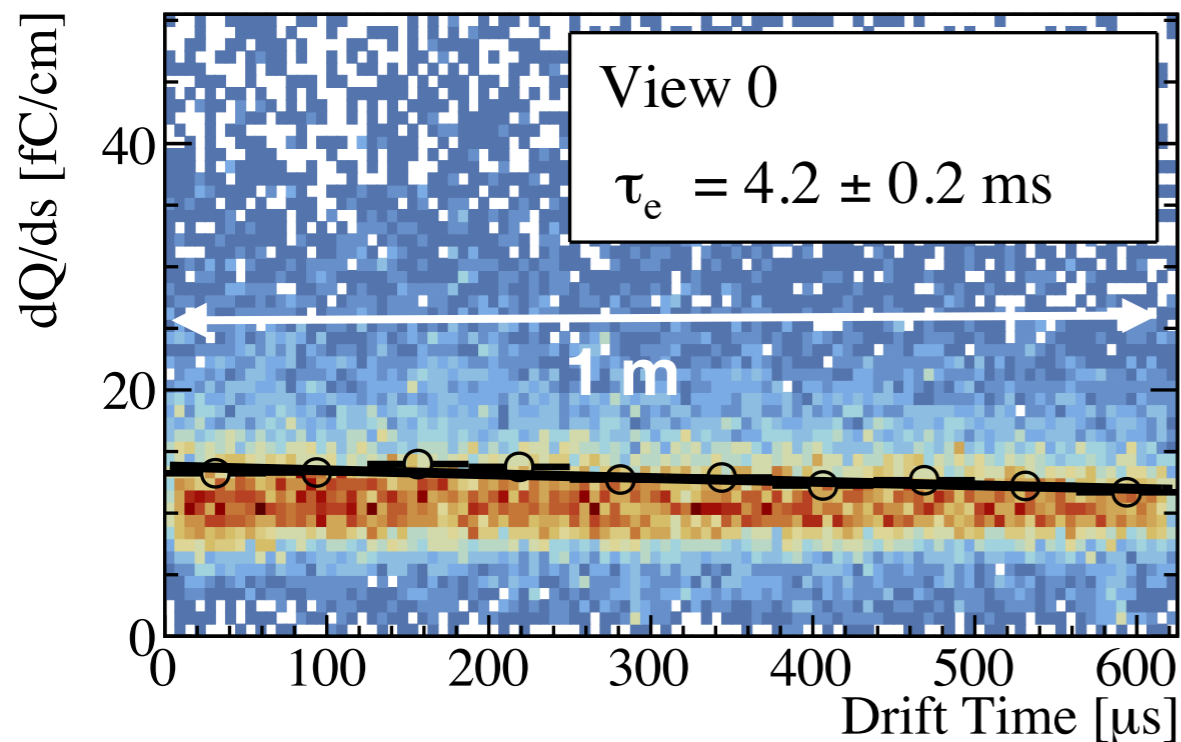
**charge is  
 equally shared  
 between views**

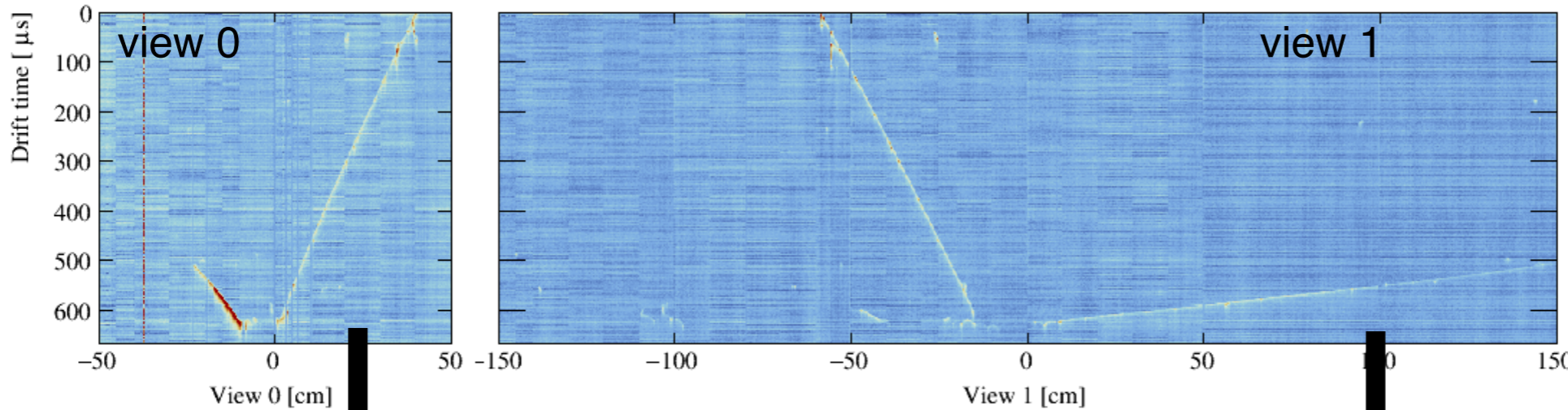


Select tracks that cross the entire 1 m drift.  
 Compute the  $dQ/dx$  as a function of drift.

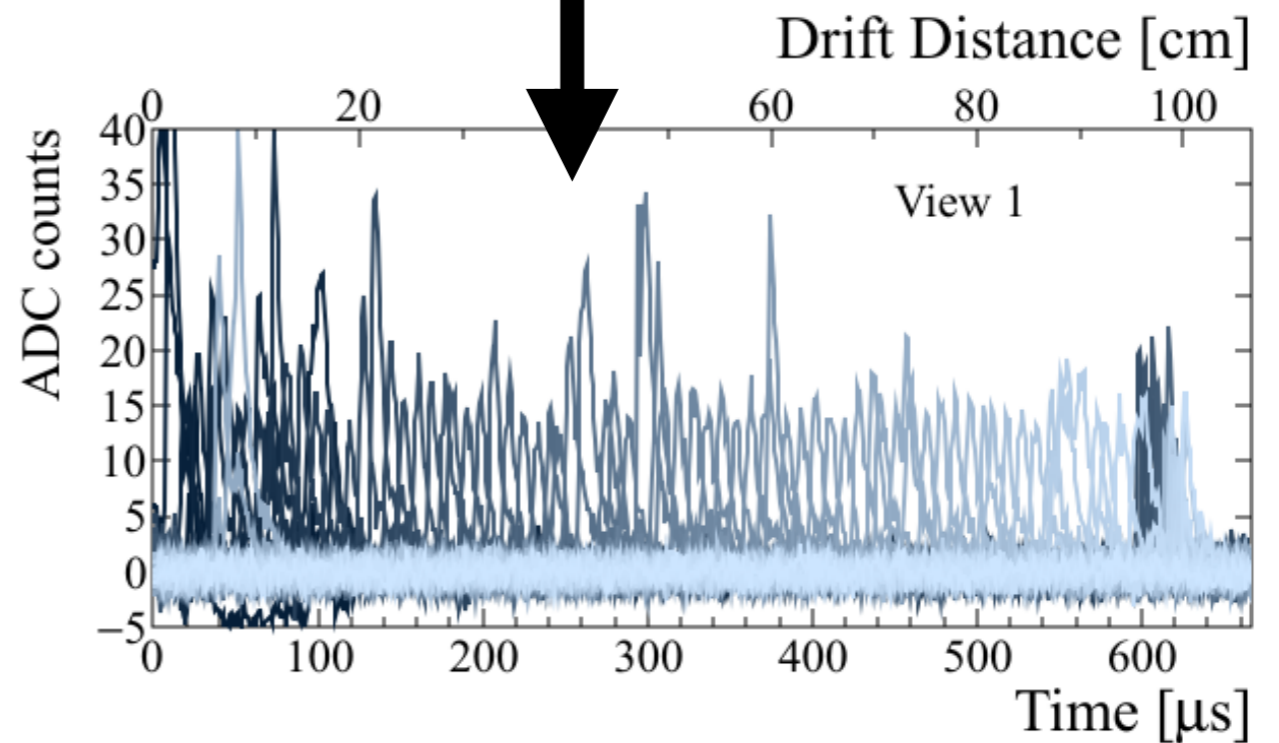
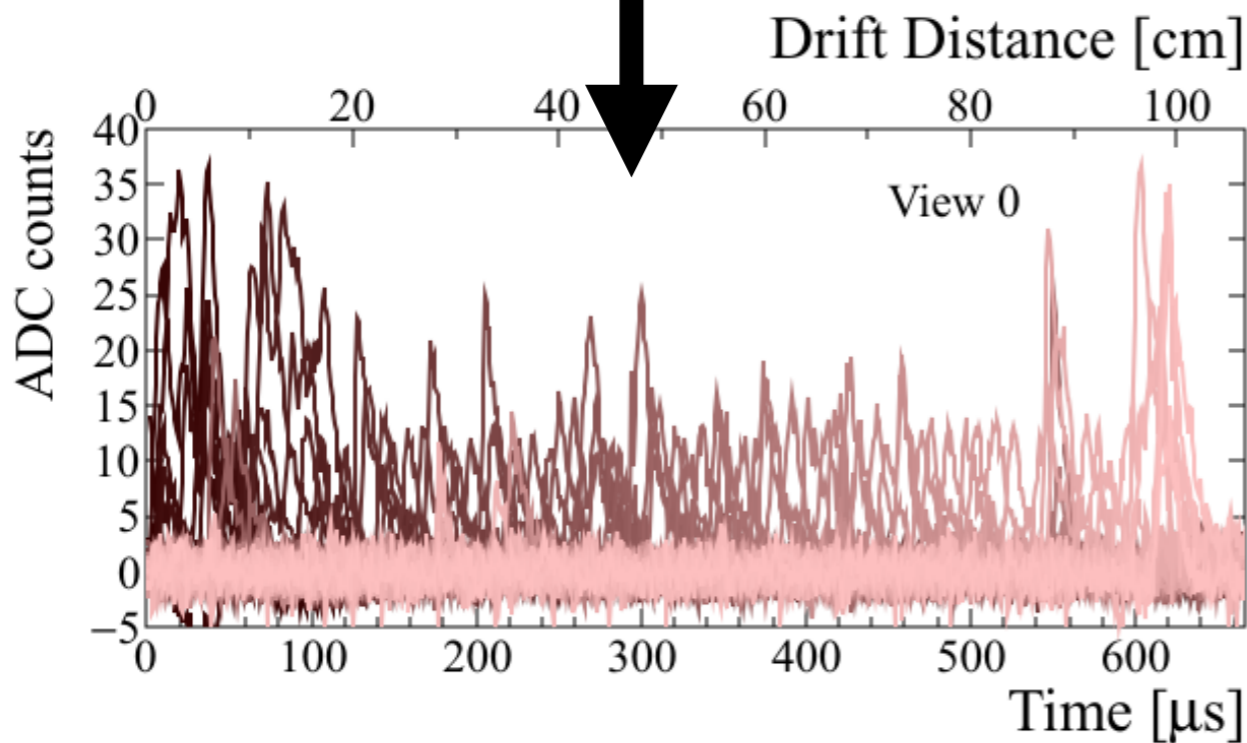
$$dQ/ds \propto e^{-t_{drift}/\tau_e}$$

✓ electron lifetime of few milliseconds achieved





selected track crosses strips at  $\phi \sim 45^\circ$ .

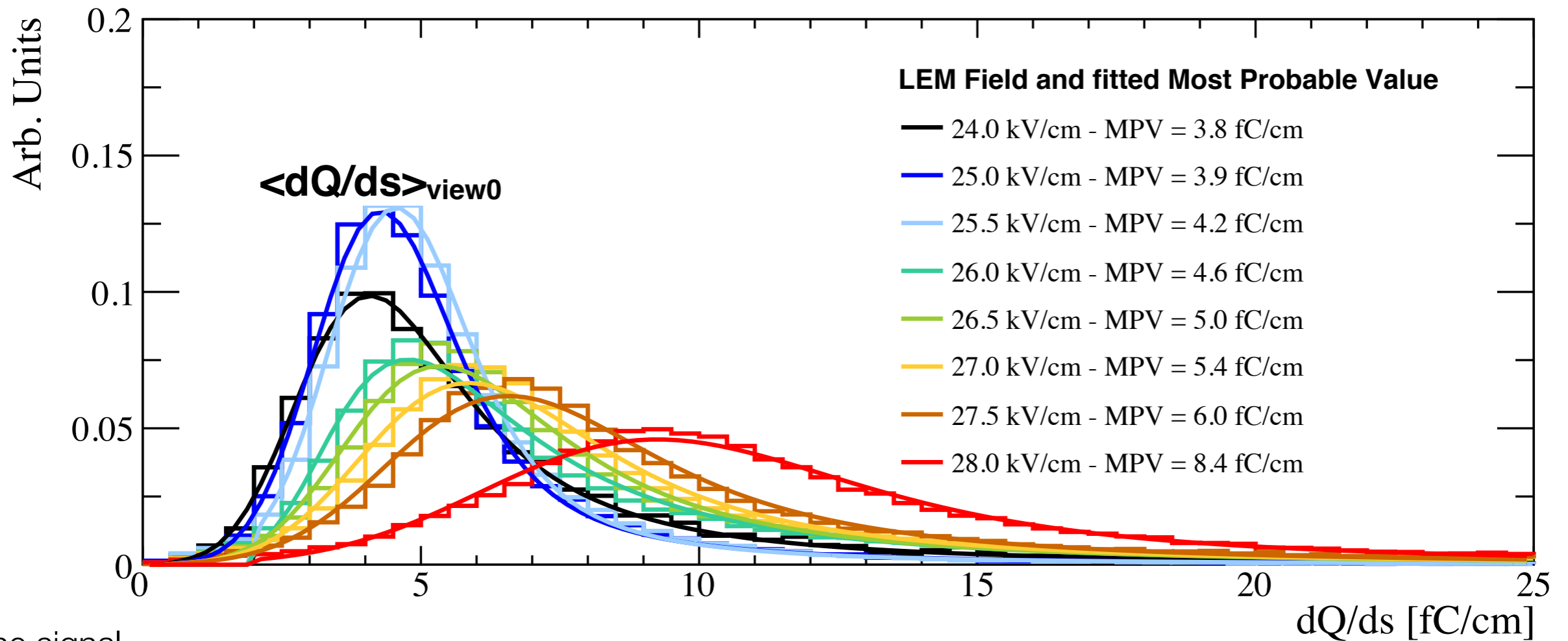


✓ Two views with **similar unipolar response**, signals well above the ambient noise.

- similar amplitudes on both views: visual confirmation 50/50 charge sharing between views



increase of the mean and MP value of the  $dQ/dx$  distributions as a function of the LEM fields. 28 kV/cm of LEM field corresponds to an operation of the 3x1x1 TPC at  $G_{\text{eff}} \approx 3$ .



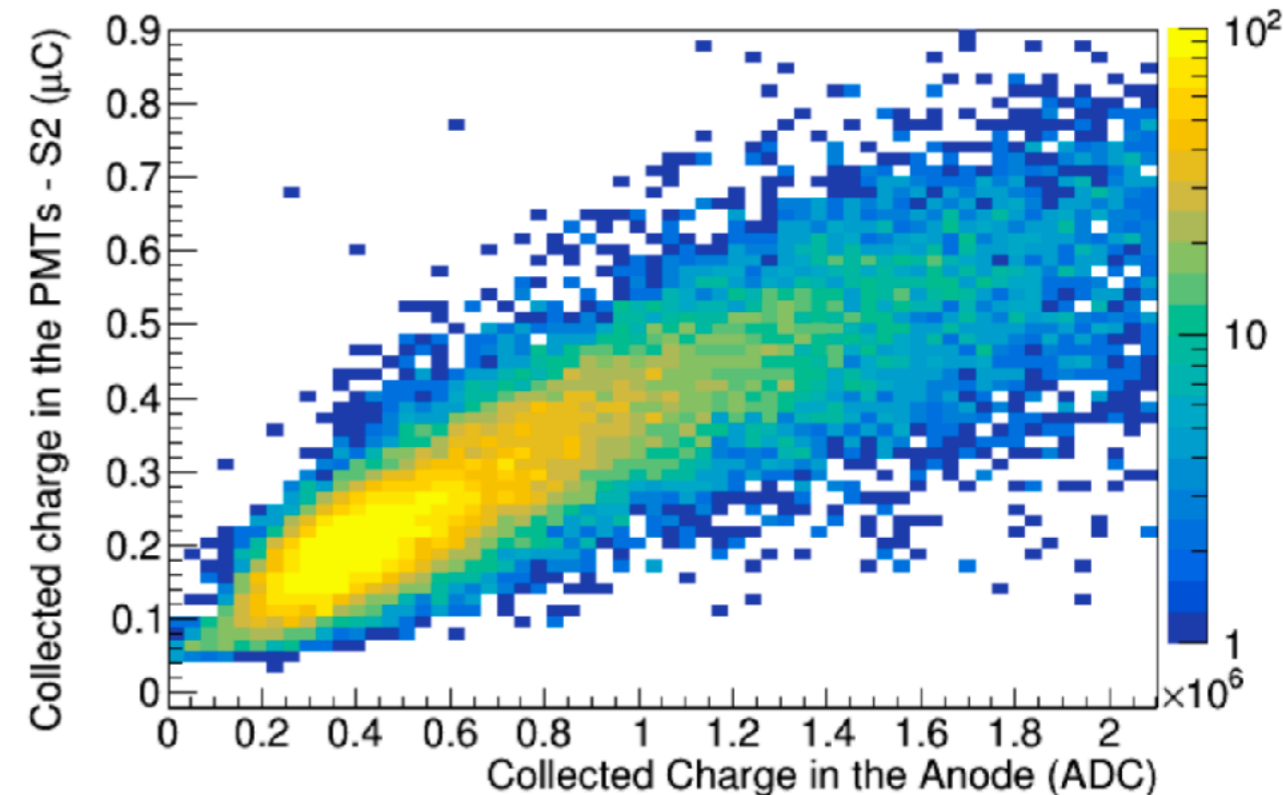
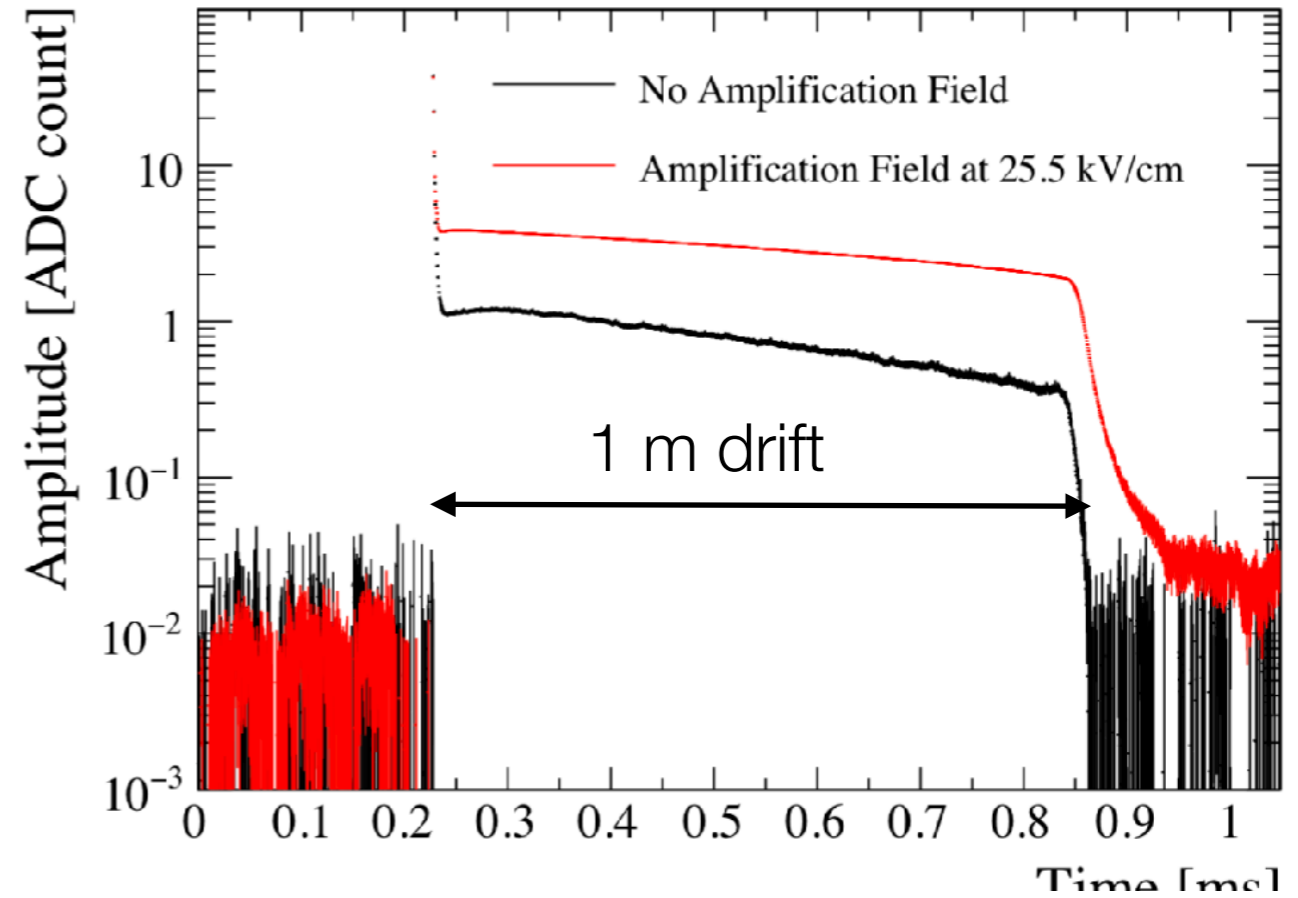
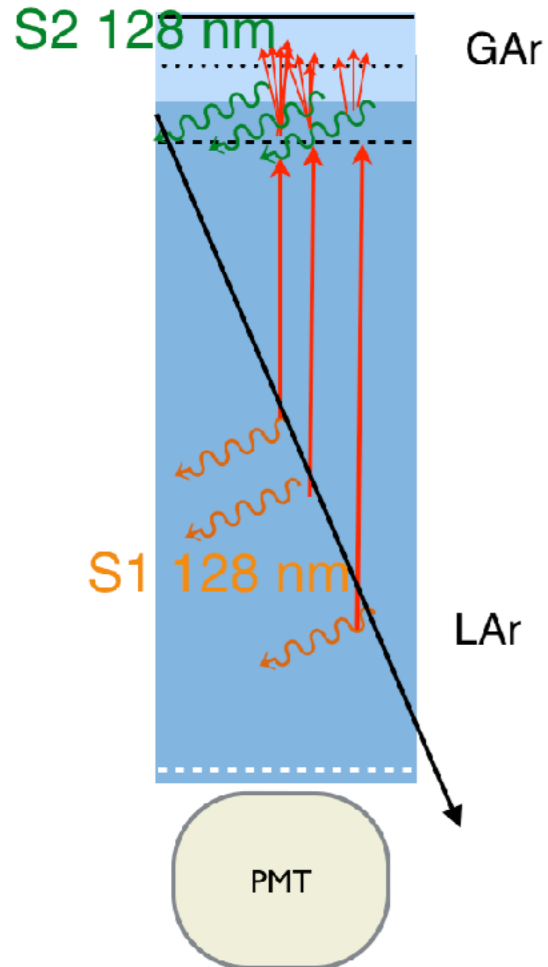
The signal measured on one view

charge sharing between views  
**50% charge sharing**

**effective gain goal 20**

**10 fC/cm** (at 500 V/cm drift)

$$\left\langle \frac{dQ}{ds} \right\rangle_{view_i} = F_{share}(view_i) \times \epsilon_{extraction} \times G_{LEM} \times \epsilon_{induction} \times \left\langle \frac{dQ}{ds} \right\rangle_{MIP}$$



- Clearly visible light from primary and secondary scintillation.
- First check of correct event matching between charge and light events. Correlation between the quantity of light and charge detected between matched events.
- Comparison between the light simulation and data.

- Despite technical issues that prevented from stably operating the TPC at  $G_{\text{eff}}$  of 20, we have demonstrated the high quality of the dual-phase TPC imaging and provided a proof of principle that such devices can be constructed and operated at the ton scale.
- A total of about **400 k high quality cosmic events retrieved in many different field configuration.**
- **Good performance of cryostat and cryogenic system:** purity compatible with ms electron lifetime and LAr level stable at sub-mm scale.
- Stable 500 V/cm drift field over one meter
- **First time ever, charge extraction over 3m<sup>2</sup> area and **LEM amplification demonstrated on 50x50 cm<sup>2</sup> modules.****
- stable performance of FE electronics, low noise and no evidence of channels dying during detector operation.

- First LAr TPC operation in a membrane tank and excellent performance of cryogenic system
- proof of stable charge extraction over a 1 cm gap on a 3 m<sup>2</sup> surface in 17m<sup>3</sup> of LAr
- First time operation of multiple side by side 50x50 cm<sup>2</sup> LEMs with gain
- Operation of an entire 3m<sup>2</sup> CRP (anode, LEM + grid) and gained a detailed understanding of the capacitive couplings between each stage.
- Many methods developed to monitor level (precision level meters, LEM-grid capacitive measurements ..)
- First time use in a LAr TPC of accessible cold front end electronics: they have shown to be robust to discharges and offer excellent noise performance even with readouts of ~500 pF (3 m strips)
- Stable operation of the drift cage with cathode at 60 kV
- excellent quality of charge readout offered by two collection views and gain.
- Noise filtering and track reconstruction, many complex “neutrino like” events, unique opportunity to test and tune reconstruction algorithms.
- light data: observation of S2 at different extraction and LEM fields, effect of purity, drift field,.. on S1. In general comparison of response with simulations to validate and tune photon propagation models for future LAr-TPCs



THANK YOU

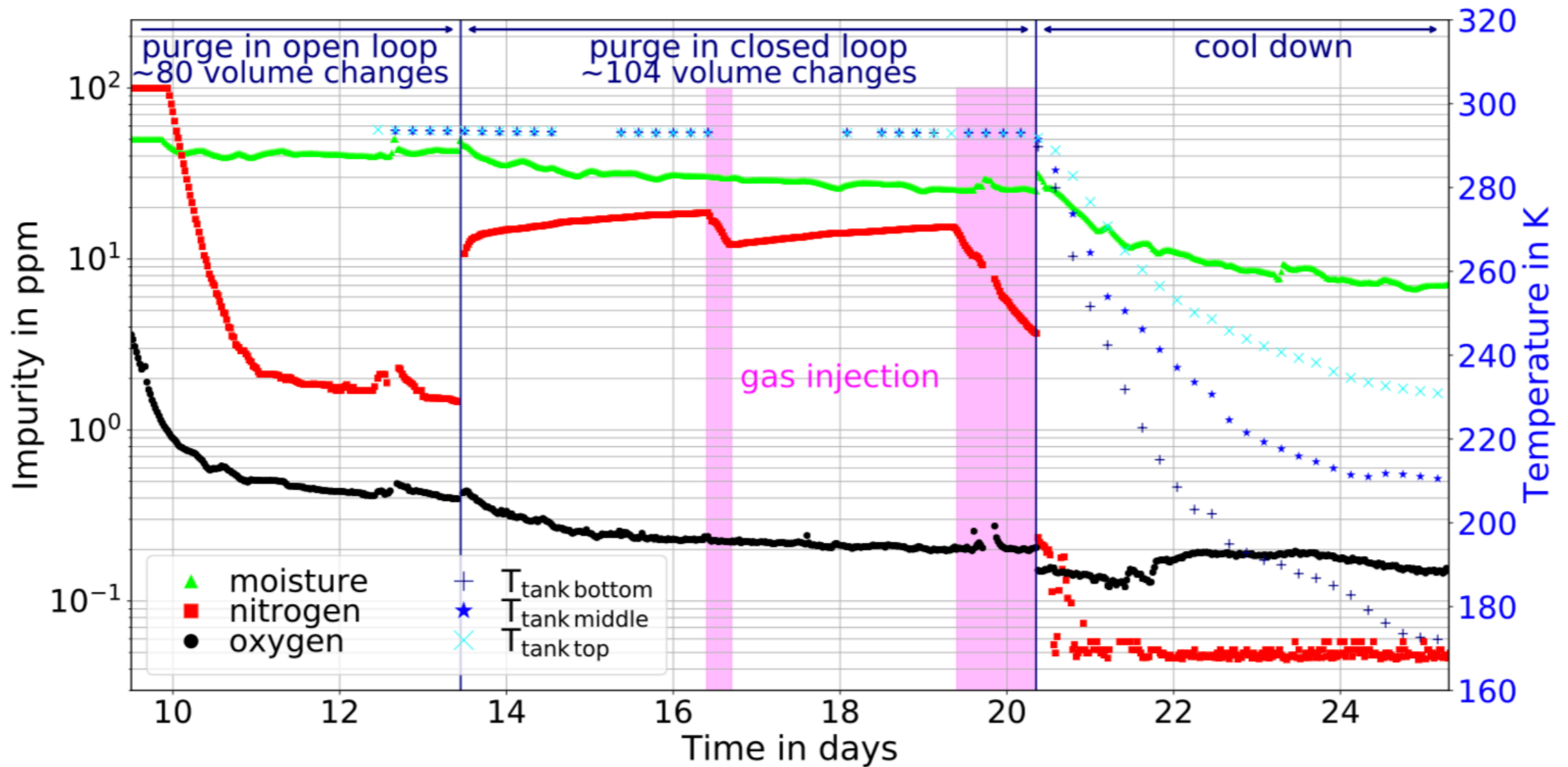
Backup

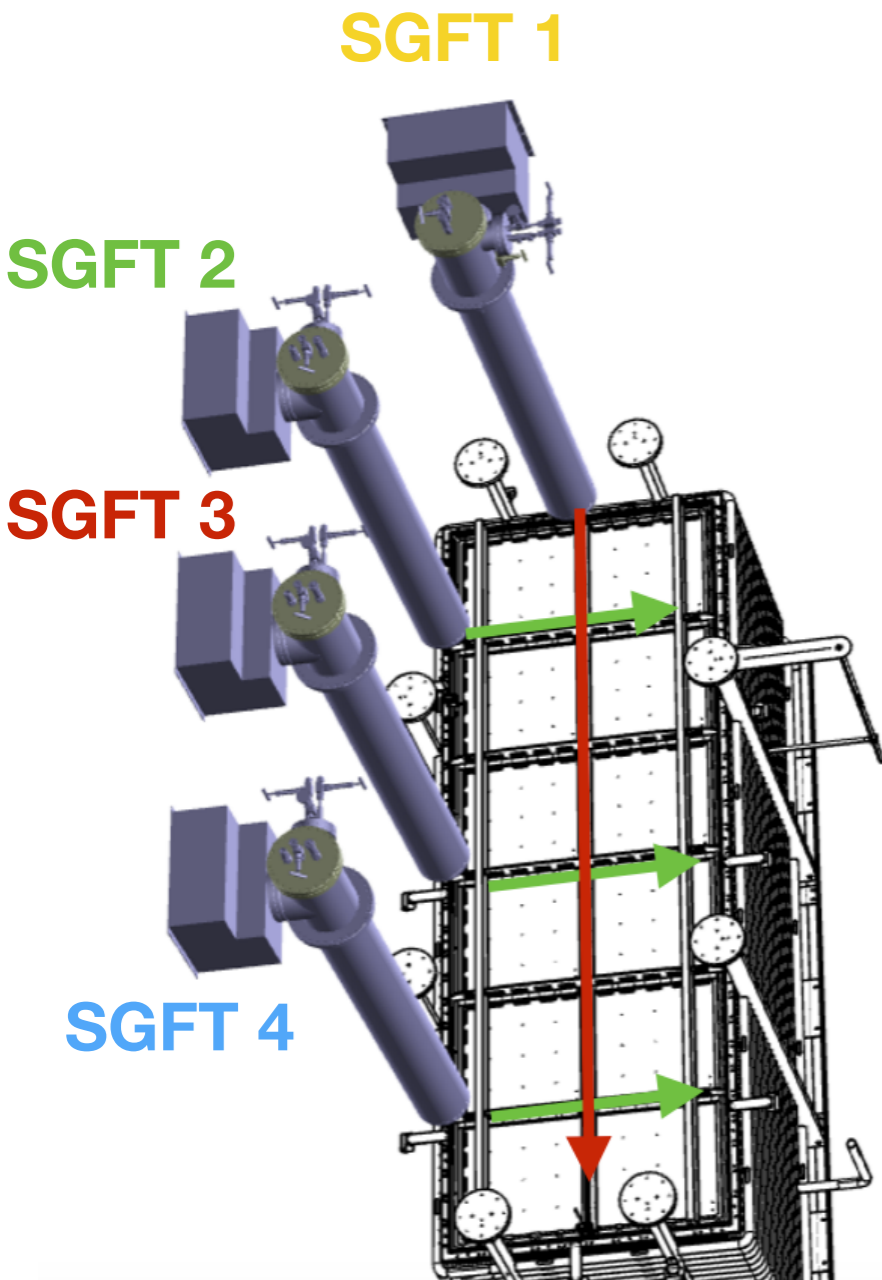
hits view 0

hits view 1

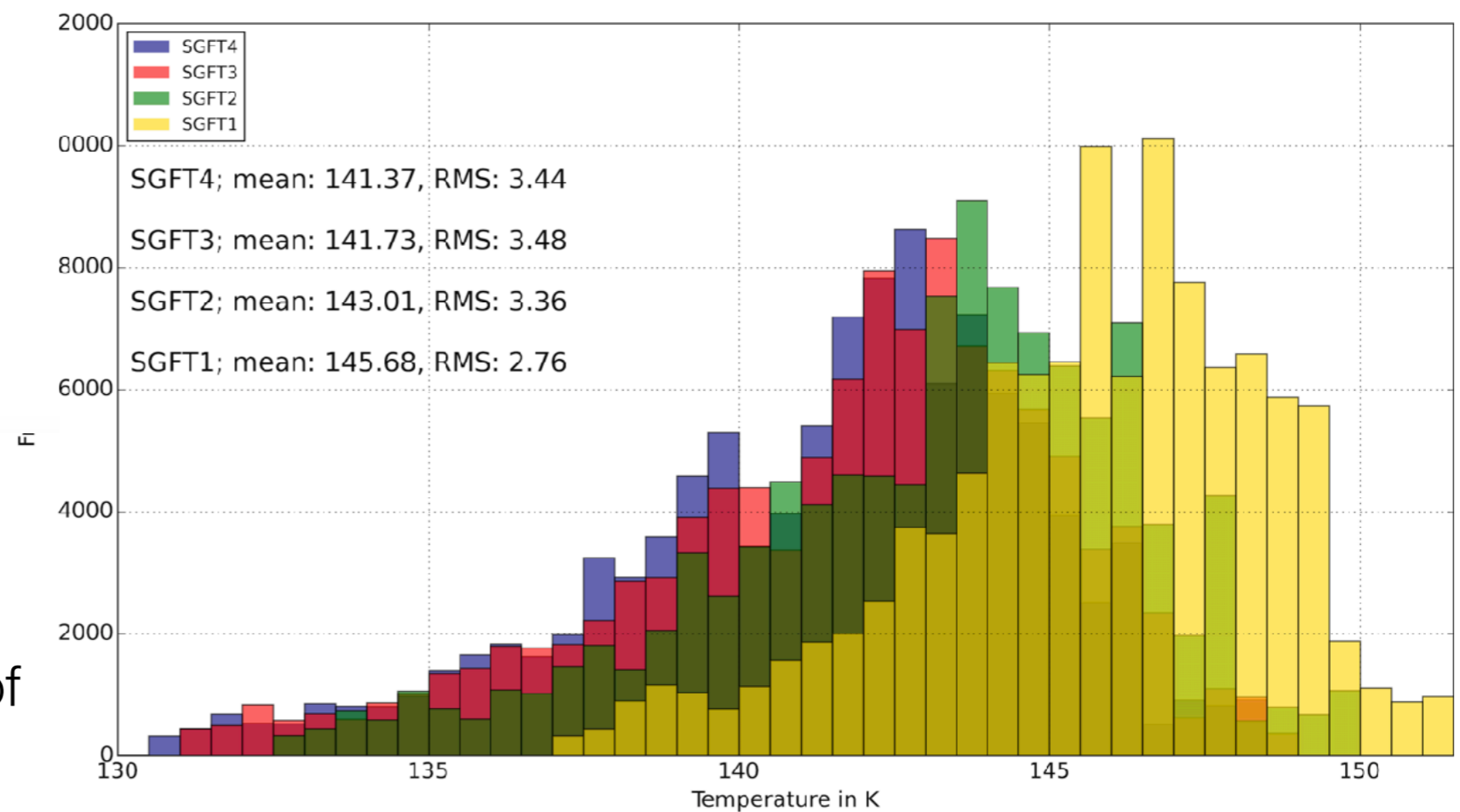
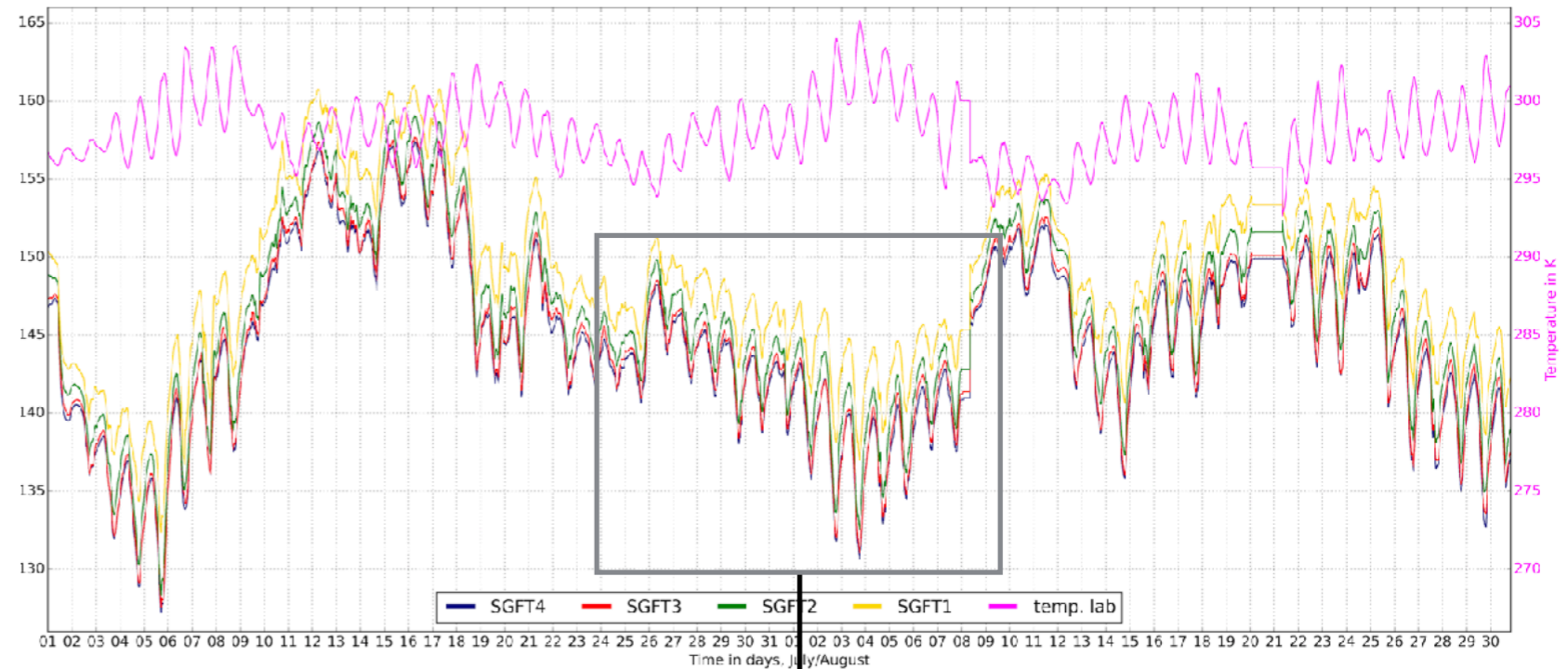
# Gas Argon evolution purity during purge

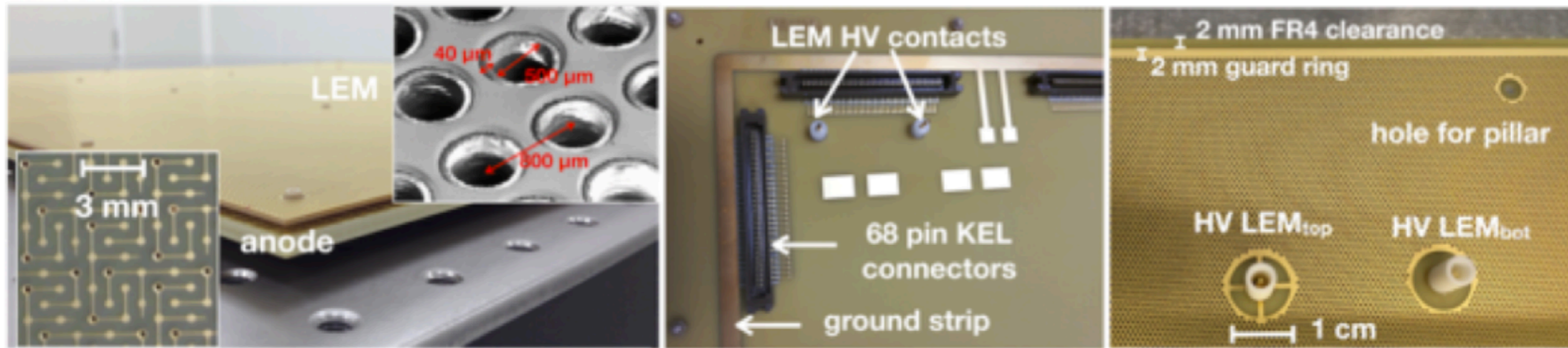
Evolution of the impurities measured in the gas during open, closed loop piston purge and cooling down. The measured temperatures inside the gas near the bottom, middle and top of the main cryostat volume are indicated in blue.





temperature FE:  $\sim 140 \pm 5$  K  
without SGFT cooling coils.  
(see Franco's slides for effect of cooling)





The system can be represented by a network of capacitively coupled electrodes including the anode, the LEM down, the LEM up, the grid and the field cage. We have measured all the involved capacitance and define a ramping up procedure where all the currents involved are adjusted taking into account the capacitive couplings.

**Table 4.** Approximate inter-electrode capacitance measured in the  $3 \times 1 \times 1 \text{ m}^3$  (see text for nomenclature).

Electrode	distance (mm)	capacitance in GAr (pF)
3 m (1 m) anode strip to GND	-	480 (160)
$50 \times 50 \text{ cm}^2$ LEM-top to anode plane	2	1000
$50 \times 50 \text{ cm}^2$ LEM-top to LEM-bot	1	7000
$50 \times 50 \text{ cm}^2$ LEM-top to neighbour LEM-top	4.5	$\leq 1$
$50 \times 50 \text{ cm}^2$ LEM-bot to extraction grid	10	150
$3 \times 1 \text{ m}^2$ cathode to GND	200	4000



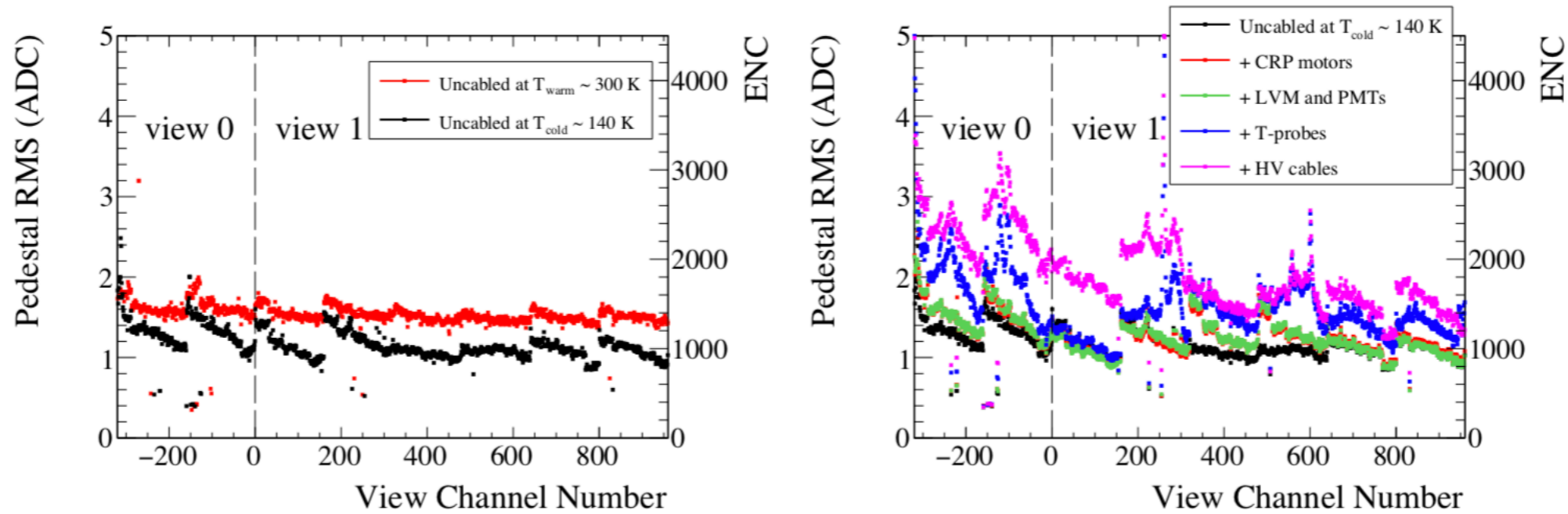


**Figure 30.** Left: comparison of noise measurements at warm (red points) and cold (black points) with the slow control cables disconnected. Right: comparison of noise measurements taken at cold by progressively reconnecting various equipment.

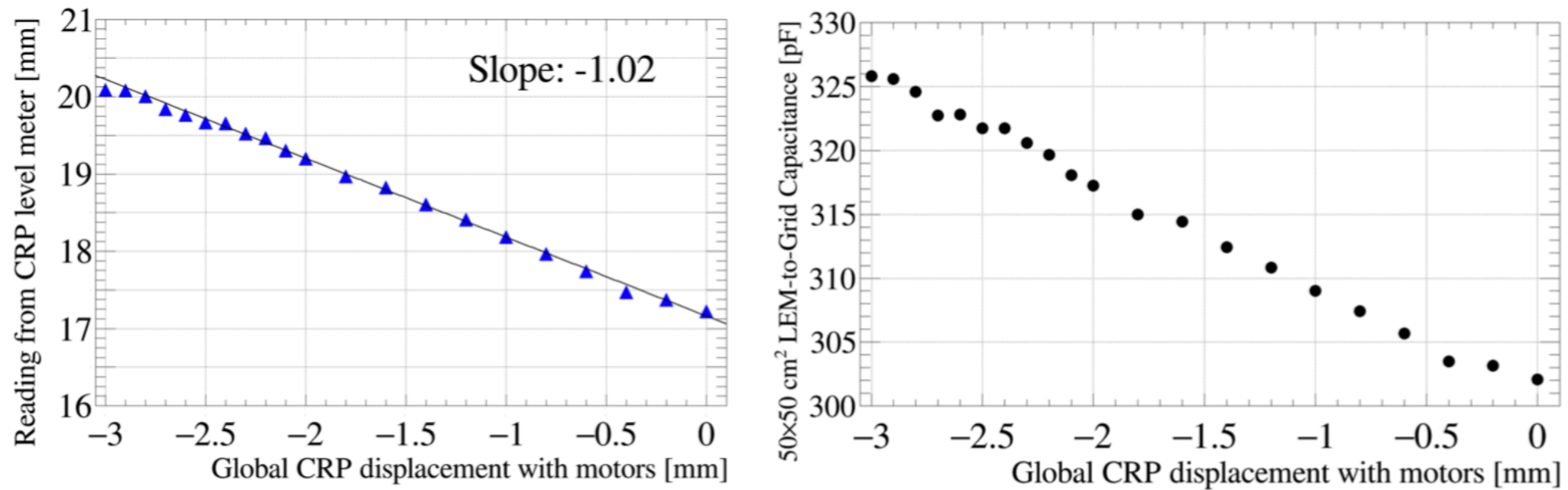
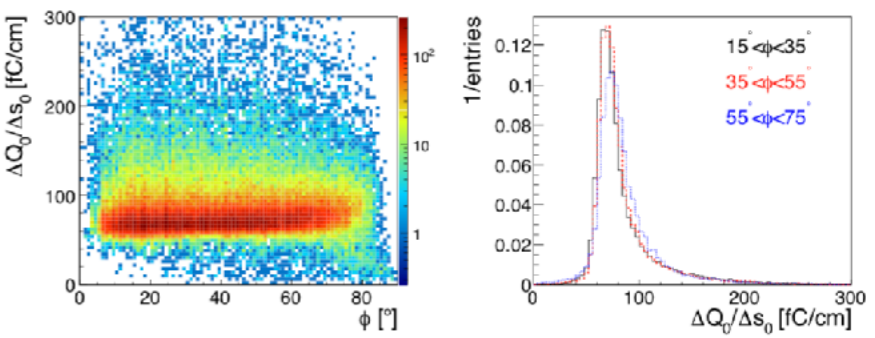
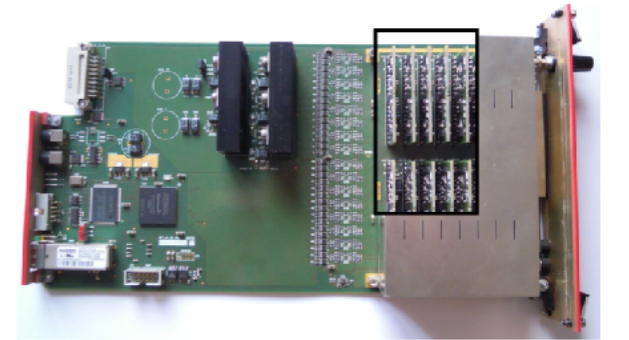
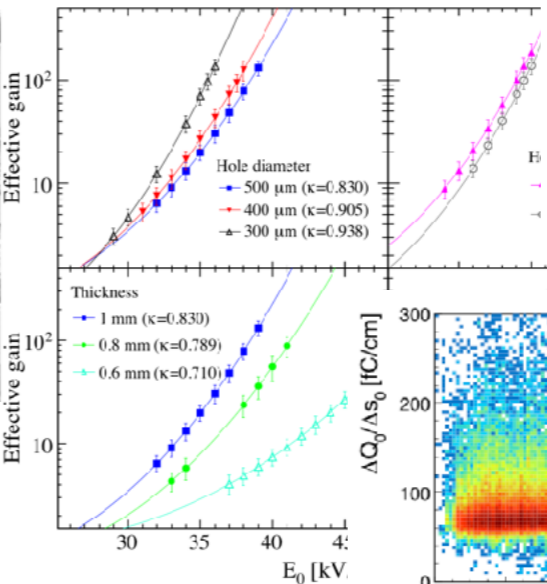
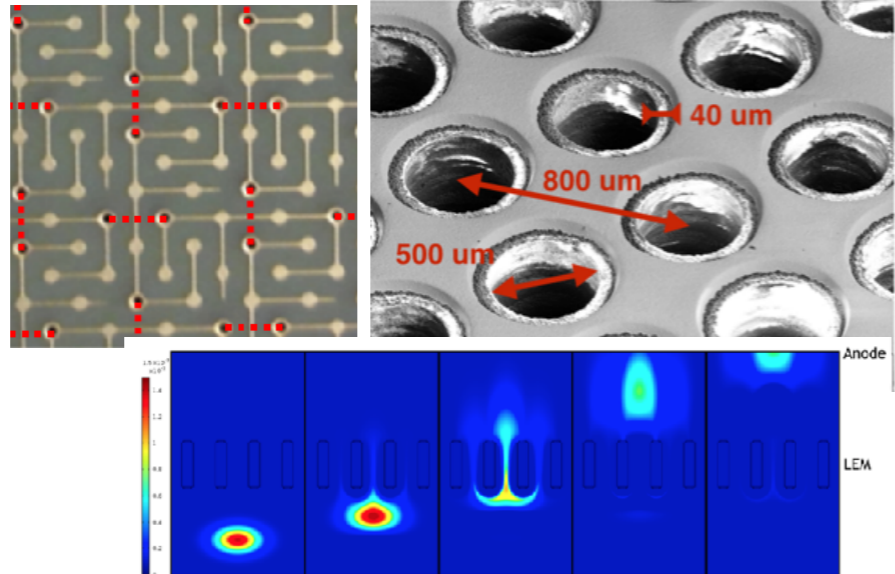
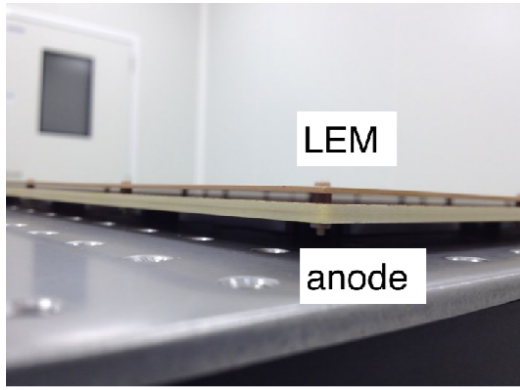


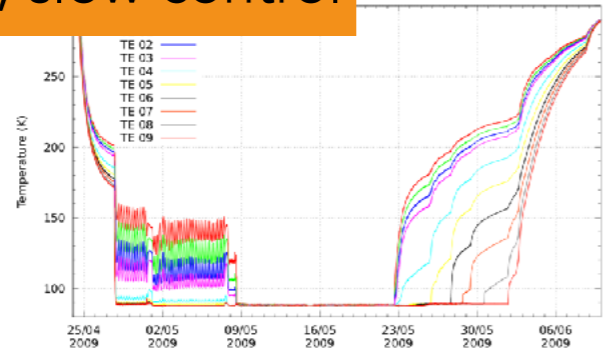
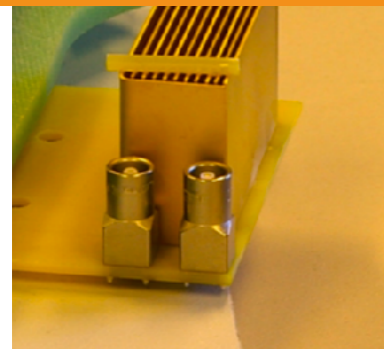
**Figure 19.** Reading from one CRP level meter (left) and  $50 \times 50 \text{ cm}^2$  LEM to extraction grid capacitance (right) as a function of the vertical position of the CRP given by the motorised system.

# Dual phase R&D prior to the 3x1x1 2005-2015

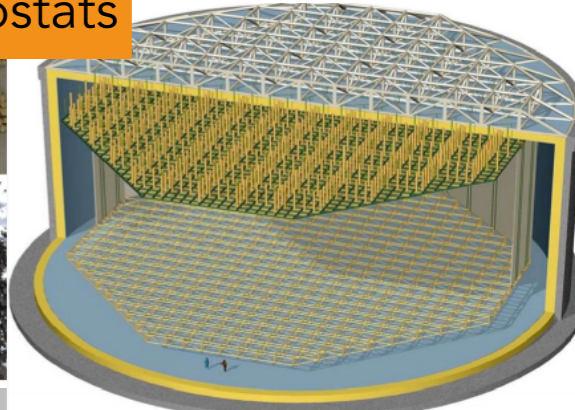
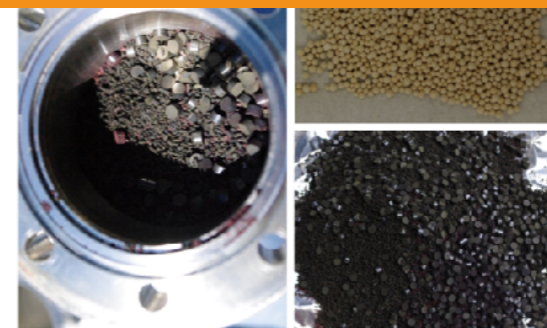
CRP: optimal design of LEMs, anodes, extraction grid, FE amplifiers



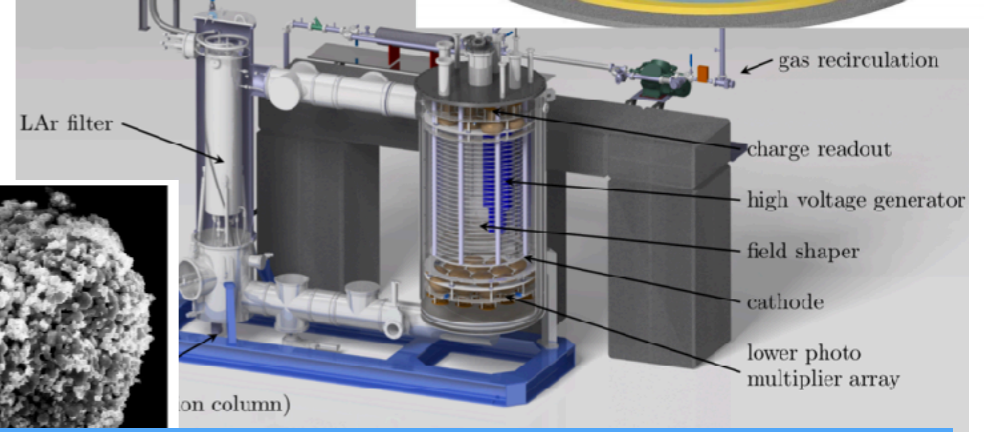
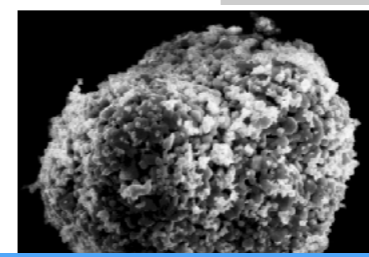
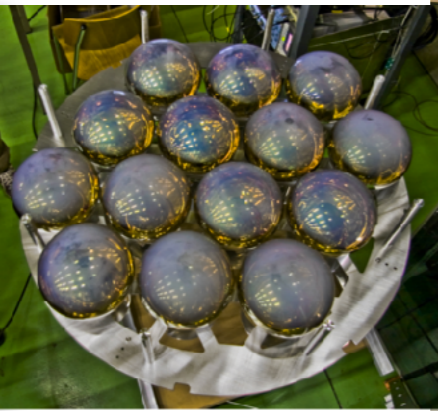
instrumentation, slow control



Cryogenics, membrane cryostats



PMTs



all components designed to be scalable to k-tonne devices